PCP
PLANT & CELL PHYSIOLOGY

SHORT AND CROOKED AWN, encoding the epigenetic regulator EMF1, promotes barley awn development

Koki Nakamura[1], Yuichi Kikuchi[1], Mizuho Shiraga[1], Toshihisa Kotake[2], Kiwamu Hyodo[1], Shin Taketa[1,*] and Yoko Ikeda[1,*]

[1]Institute of Plant Science and Resources, Okayama University, 2-20-1 Chuo, Kurashiki, 710-0046 Japan, [2]Graduate School of Science and Engineering, Saitama University, 255 Shimo-Okubo, Sakura-ku, Saitama, 338-8570 Japan

*Corresponding author: E-mail, staketa@rib.okayama-u.ac.jp, yikeda@okayama-u.ac.jp

Received 10 September 2024; Accepted 20 December 2024

Abstract

The awn is a bristle-like extension from the tip of the lemma in grasses. In barley, the predominant cultivars possess long awns that contribute to grain yield and quality through photosynthesis. In addition, various awn morphological mutants are available in barley, rendering it a useful cereal crop to investigate the mechanims of awn development. Here, we identified the gene causative of the *short and crooked awn* (*sca*) mutant, which exhibits a short and curved awn phenotype. Intercrossing experiments revealed that the *sca* mutant induced in the Japanese cultivar (cv.) "Akashinriki" is allelic to the independently isolated moderately short-awn mutant *breviaristatum-a* (*ari-a*). Map-based cloning and sequencing revealed that *SCA* encodes the Polycomb group–associated protein EMBRYONIC FLOWER 1. We found that SCA affects awn development through the promotion of cell proliferation, elongation, and cell wall synthesis. RNA sequencing of cv. Bowman backcross-derived near-isogenic lines of *sca* and *ari-a6* alleles showed that SCA is directly or indirectly involved in promoting the expression of genes related to awn development. Additionally, SCA represses various transcription factors essential for floral organ development and plant architecture, such as MADS-box and Knotted1-like homeobox genes. Notably, the repression of the C-class MADS-box gene *HvMADS58* by SCA in awns is associated with the accumulation of the repressive histone modification H3K27me3. These findings highlight the potential role of SCA-mediated gene regulation, including histone modification, as a novel pathway in barley awn development.

Keywords: barley; awn development; EMBRYONIC FLOWER 1 (EMF1); homeotic genes; H3K27 trimethylation; epigenetic regulation

Introduction

Barley (*Hordeum vulgare* L.) is an important cereal crop and one of the oldest domesticated crops. Awns are crucial for barley; they play various roles in wild and agricultural settings. In wild grass species, awns aid seed dispersal and deter predation, whereas in cultivated barley, they contribute to photosynthesis, increasing grain yield (Grundbacher 1963, Kjack and Witters 1974, von Bothmer et al. 1995). Because of the functional advantages provided by barley awn, most domesticated barley varieties retain long awns. Conversely, many rice (*Oryza sativa*) varieties have lost their awns, primarily for ease of sowing and storage (Takahashi 1955). Given the unique characteristics and important physiological functions of barley awns, it is crucial to understand the molecular basis of their development.

Several genes and pathways involved in awn morphology have been identified in grass species, which has deepened our understanding of awn development. In rice, several genes controlling awn development have recently been characterized, for example, *Awn-1* (*An-1*)/*REGULATOR OF AWN ELONGATION 1* (*RAE1*), encoding a basic helix-loop-helix (bHLH) transcription factor (TF); *RAE2*/*GRAIN LENGTH AND AWN DEVELOPMENT1* (*GAD1*), encoding EPIDERMAL PATTERNING FACTOR like protein 1; and *RAE3*, encoding RING-type E3 ubiquitin ligase, which positively regulate awn development (Luo et al. 2013, Bessho-Uehara et al. 2016, 2023). *LONG AND BARBED AWN 1* (*LABA1*)/*An-2*, which encodes a cytokinin-activating enzyme, is involved in the development of long and barbed awns in wild rice (Gu et al. 2015, Hua et al. 2015). Additionally, the YABBY family TF *DROOPING LEAF* (*DL*), a *CRABS CLAW* (*CRC*) ortholog in *Arabidopsis*, promotes rice awn development in a noncell-autonomous manner (Toriba and Hirano 2014).

Plant And Cell Physiology, 2025, 66(5), 705–721
doi:https://doi.org/10.1093/pcp/pcae150
Advance Access publication on 20 December 2024

Meanwhile, the YABBY family TF *TONGARI-BOUSHI1* (*TOB1*) maintains proper meristem organization in rice spikelets and suppresses awn development (Tanaka et al. 2012). In wheat (*Triticum aestivum* L.), *B1*, encoding a C2H2 zinc finger protein with EAR motifs, is known to inhibit awn development (DeWitt et al. 2020, Huang et al. 2020). The wheat *FRIZZY PANICLE* (*WFZP*), which encodes a Class II AP2/ERF TF, promotes awn elongation and suppresses spikelet formation (Du et al. 2021). In sorghum (*Sorghum bicolor*), *AWN1*/*DOMINANT AWN INHIBITOR* (*DAI*), which encodes an ALOG protein, inhibits awn elongation (Zhou et al. 2021, Takanashi et al. 2022).

In barley, various awn-related mutants have been isolated (Liller et al. 2017, Huang et al. 2021). *SHORT AWN 2* (*Lks2*), encoding a SHORT INTERNODE family TF, is involved in awn elongation and pistil morphology (Yuo et al. 2012). Barley *APETALA2* (*HvAP2*)/*Cleistogamy1* (*Cly1*)/*ZEOCRITON1* (*Zeo1*) promotes floret identity and the formation of outer floral organs, including awn elongation (Anwar et al. 2018, Patil et al. 2019). *HvMADS1*, encoding the SEPALLATA (SEP) TF, forms a complex with HvAP2 to activate *Lks2* and *HvDL*, promoting awn elongation (Li et al. 2021, Zhang et al. 2024). The *Hooded (Kap)* mutant exhibits the extra floret of inverse polarity on the lemma, which is caused by the ectopic overexpression of the barley Knotted1-like homeobox (KNOX1) gene *Bkn3*/*HvKNOX3* in the awn (Müller et al. 1995). Many barley awn mutants exhibit simple Mendelian inheritance; therefore, barley is an excellent organism for genetic studies on awn development. However, for some loci associated with awn-related traits in barley, the specific factors have not yet been identified, and the mechanisms governing awn development in barley remain incompletely described.

In this study, we focused on the barley *short and crooked awn* (*sca*) mutant of cv. Akashinriki (Fig. 1a, Supplementary Fig. S1) induced by Konishi et al. (1984). By intercrossing, we revealed that *sca* is allelic to *ari-a* short-awn mutants independently induced in the cvs. Bonus, Foma, and Kristina (Kucera et al. 1975). We describe the morphological and biochemical characteristics of the *sca* and *ari-a6* Bowman (BW) backcross-derived near-isogenic lines (NILs; Fig. 1b, Supplementary Fig. S2a). A map-based cloning approach revealed that the causal gene for *sca* was the ortholog of the *EMBRYONIC FLOWER 1* (*EMF1*) gene, which has been reported to function in cooperation with the polycomb repressive complex (PRC) to mediate gene repression (Sung et al. 1992, Calonje et al. 2008, Yan et al. 2015, Zheng et al. 2015). *Arabidopsis* EMF1 maintains vegetative development through suppressing flowering (Sung et al. 1992). In rice, EMF1 determines palea identity and supports development of inner floral organs (Yan et al. 2015, Zheng et al. 2015). In contrast, we noticed that *sca* mutations of barley exhibit severely reduced awns without affecting palea morphology. These remarkable phenotypic differences indicate the divergence of *SCA* from the rice ortholog. Additionally, we characterized SCA's role in promoting cell proliferation, elongation, and cell wall biosynthesis. We revealed that SCA is involved in the gene repression though H3K27me3 deposition and acts as a key regulatory factor for awn development in barley.

Results

Short-awn mutants, *sca* and *ari-a*, are allelic and exhibit similar phenotypes

We assessed the phenotype of the *sca* (OUM206) mutant, which was induced by treating cv. Akashinriki with ethyl methanesulfonate (Konishi et al. 1984). Compared with wild-type Akashinriki, the *sca* mutant showed a 59% reduction in awn length and a 6% decrease in culm length; moreover, awn tips in the upper part of the spike were curved (Fig. 1a, Supplementary Fig. S1). The *uzu* semidwarfism of Akashinriki is known to be caused by mutation of the brassinosteroid receptor *BRASSINOSTEROID-INSENSITIVE 1* (*BRI1*; Chono et al. 2003). For better awn phenotyping, we also used the BW backcross-derived near-isogenic line *sca*-BW in which the *sca* gene was introduced onto the genetic background of BW. This approach was taken because BW has long awns but no semidwarfism gene (Fig. 1b, d, Supplementary Fig. S2a; Druka et al. 2011). The awns in *sca*-BW were found to be extremely short and thin, but the awn tips did not curve, unlike the *sca* mutant in Akashinriki (Fig. 1a, b). The awn tips of the *sca* mutant bend likely because the awns on six-row dense spikes receive rubbing force from surrounding flag leaf sheaths during spike extrusion, while the very short awns of *sca*-BW on two-row slender spikes could extrude smoothly because they receive less friction from the flag leaf sheaths. Additionally, the induced short-awn *ari-a* mutant panel, comprising 27 allelic mutants derived from three Nordic barley cultivars (Kucera et al. 1975), was also observed because this panel's map location on the 3HS arm was similar to that of *sca*. The *ari-a* mutants generally had short and thin awns that exhibited bending, but their awn phenotypes varied among the lines (Fig. 2a–c). Of these, *ari-a.6* allele was available as a BW backcross-derived near-isogenic line (*ari-a.6*-BW; Fig. 1b, Supplementary Fig. S2A). The awns of *ari-a.6*-BW were curved unlike those of *sca*-BW (Fig. 1b). The *ari-a.6*-BW has approximately two times longer awns compared with *sca*-BW that are more prone to bending due to increased contact with surrounding structures. Next, an allelism test was performed through intercrossing *ari-a.6*-BW and *sca*-BW. F_1 plants had short and thin awns, which drooped and curved (Supplementary Fig. S2B). The awn morphology of F_1 plants was more similar to that of *sca*-BW. From these findings, we confirmed that *sca* and *ari-a.6* are allelic.

We also investigated the phenotypic traits of *sca*-BW and *ari-a.6*-BW under field conditions for 2 years. *sca*-BW and *ari-a.6*-BW consistently exhibited shorter awns and culms than BW (Fig. 1d, Supplementary Fig. S2C, Supplementary Table S1). Furthermore, the *sca*-BW showed particularly severe agronomic defects, including reduced grain number and weight, and delayed heading time (Supplementary Table S1). Additionally, the seed fertility of both mutant NILs was lower than that of BW. The spike length and number of spikelets per spike were

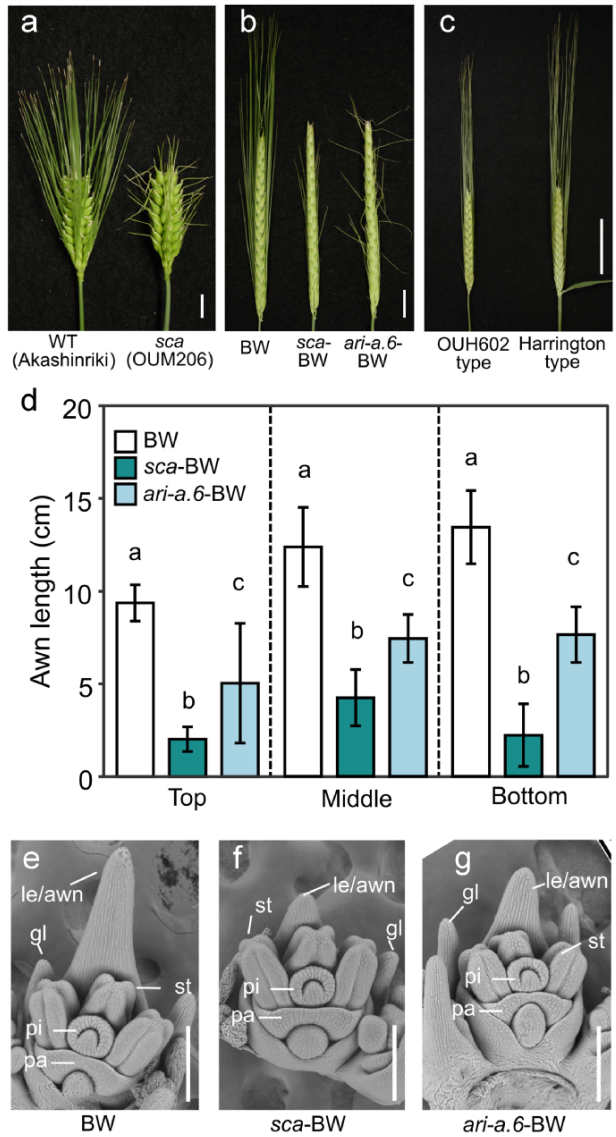

Figure 1. Short-awn phenotype of *sca* and *ari-a* mutants and natural variation. (a) Spikes of wild type (cv. Akashinriki, WT) and *sca* (OUM206) plants. Bar = 1 cm. (b) Spikes of BW (left) and BW near-isogenic lines (NILs), *sca*-BW (middle) and *ari-a.6*-BW (right). Bar = 1 cm. (c) Spikes of typical cv. Harrington (long) and OUH602 (short) awn-type BC_1F_2 plants segregated in the progeny of a heterozygous Harrington/OUH602//Harrington backcross plant selected by genotyping of the *sca*-flanking marker. Bar = 5 cm. (d) The awn lengths of BW, *sca*-BW, and *ari-a.6*-BW in 2019 under field conditions. The lengths of the awn extending from the fourth spikelet from the top (Top), from the spikelet in the middle (Middle), and from the fourth spikelet from the bottom (Bottom) are shown. Error bars, ±SD ($n = 8$ plants). Distinct letters indicate significant differences as determined by the Tukey–Kramer test ($P < 0.01$). Spikelets at the initiation stage of awn elongation (corresponding to Waddington scale W4.5) in BW (e), *sca*-BW (f), and *ari-a.6*-BW (g). Bar = 200 μm. Abbreviations: gl, glume; le, lemma; ov, ovule; pa, palea; pi, pistil; st, stamen; stig, stigma.

significantly reduced for mutant NILs in 2020. Taking these results together, it is indicated that SCA positively regulates awn elongation and enhances grain yield in the field.

SCA affects awn development by promoting cell proliferation, cell elongation, and cell wall synthesis

To determine whether SCA is involved in awn development from the initiation of awn primordia, we observed spikelets at Waddington stage W4.5 in BW, *sca*-BW, and *ari-a.6*-BW using scanning electron microscopy (SEM; Fig. 1e–g; Waddington et al. 1983). The awn primordium was notably smaller in both mutant NILs than in BW, particularly in *sca*-BW, indicating that SCA contributes to awn elongation as early as the primordium stage corresponding to W4.5.

Next, hand sections of the middle part of the awns were observed microscopically 2 weeks after heading for BW and *ari-a.6*-BW (Fig. 3a–d). *sca*-BW awn was excluded from the analysis because its thinness and shortness made hand sectioning

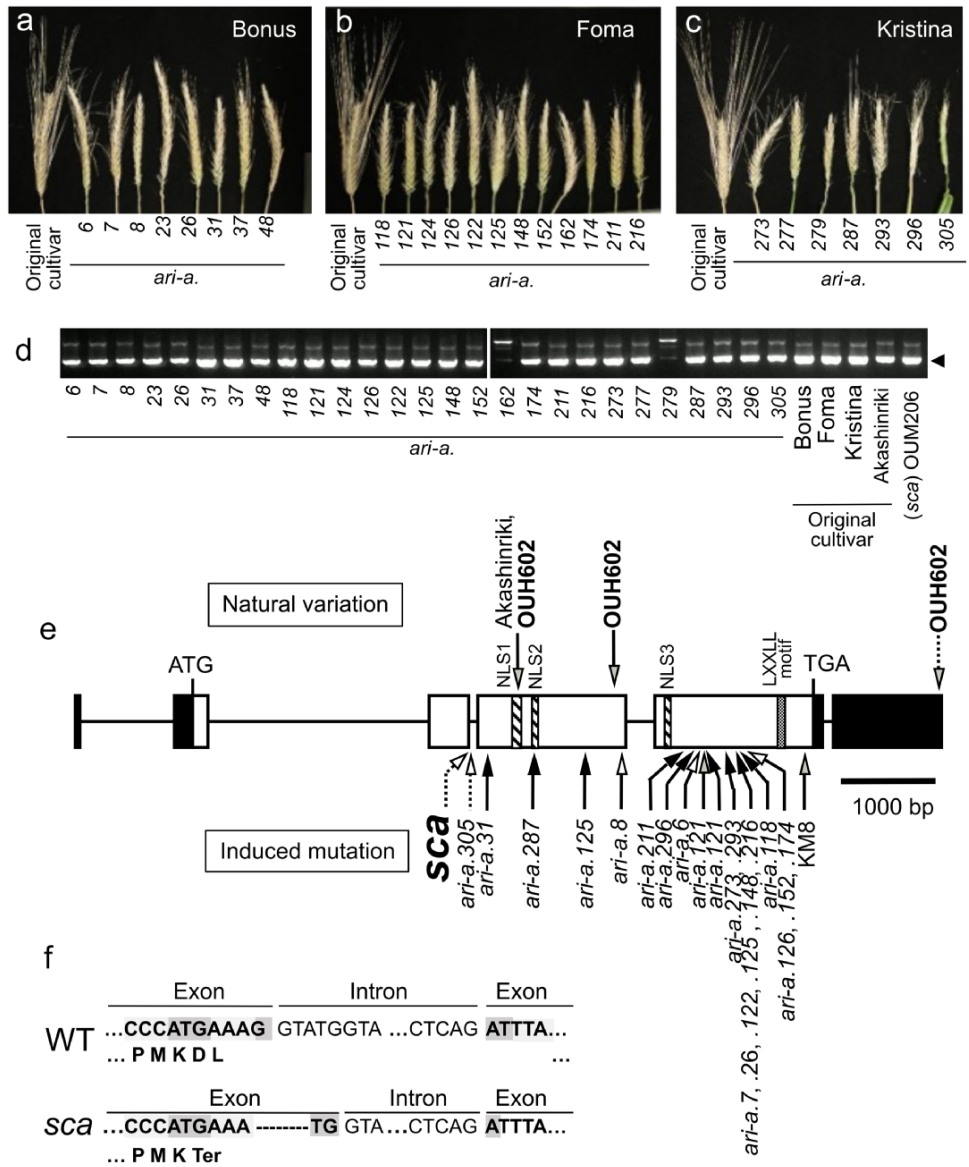

Figure 2. Identification of the *SHORT AND CROOKED AWN* (*SCA*) gene. (a–c) Spikes of the original barley cultivars and *ari-a* mutants. Mutants of cv. Bonus (a), cv. Foma (b), and cv. Kristina (c) backgrounds. Wild-type spikes are shown on the left of each image, and numbers below the spikes show the *ari-a* allele number. (d) PCR amplification results of the genomic region spanning the translation start and stop sites of *HORVU.MOREX.r3.3HG0248910* in the *ari-a* panel, *sca* (OUM206), and their original cultivars. No target band amplification was observed in *ari-a.162* and *ari-a.279*. Arrowheads indicate the target amplification product. (e) Mutation sites of 23 induced mutants (up arrows; *sca*, *ari-a* panel, and KM8) and natural variation sites (down arrows; Akashinriki and OUH602) on *HORVU.MOREX.r3.3HG0248910*. The exon/intron structure (black boxes/black lines, respectively) and transcribed regions (white boxes) are illustrated. Black solid arrows denote nonsense mutations. White solid arrows indicate frameshift mutations resulting in truncated proteins. White dotted arrows signify altered splicing due to nucleotide substitutions or deletions at exon–intron boundaries. Gray solid arrows represent missense mutations. A gray dotted arrow indicates a nucleotide substitution in the 3′-UTR region. Putative nuclear localization signals (NLSs) and the position of the LXXLL motif within the gene's translated region are marked with boxes. (f) Detailed 4-base deletion site in *sca* mutant at the exon/intron boundary of the *SCA* coding region. The 4-base deletion causes a shift in the splicing site, altering the exon–intron junction and resulting in a premature stop codon, as confirmed through the RNA-seq mapped reads of *sca*-BW (refer to Supplementary Fig. S6).

impossible. In transverse sections, both genotypes exhibited a triangular appearance with three vascular bundles and two pillars of chlorenchyma cells (Fig. 3a–d). However, *ari-a.6*-BW exhibited thinner awns and shorter parenchyma cell size in transverse and longitudinal dimensions than BW (Fig. 3e–g). The estimated number of longitudinal parenchyma cells also decreased (Fig. 3h). These findings indicate that SCA influences cell division and size in the awn. The awns of *ari-a.6*-BW

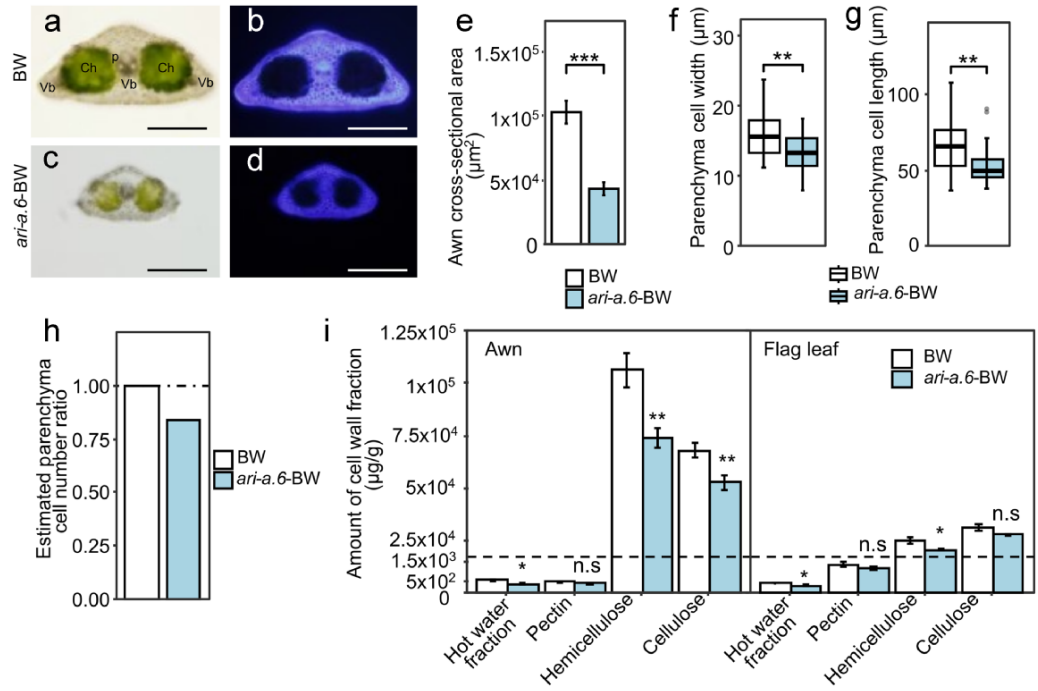

Figure 3. The effects of the *ari-a.6* mutation on awn morphology and cell wall composition. (a–d) Observation of awn cross-sections of BW and *ari-a.6*-BW. BW awn under a bright field (a); BW awn under UV light (b); *ari-a.6*-BW awn under a bright field (c); and *ari-a.6*-BW awn under UV light (d). p, parenchymal cells; vb, vascular bundle; ch, chlorenchymal tissue. Bar = 200 μm. (e) Comparison of awn cross-sectional area between BW and *ari-a.6*-BW. Error bars, ±SD ($n = 3$ awns). Student's *t*-test was used for statistical analysis (***, $P \leq 0.001$). (f) Parenchymal cell width in the cell file adjacent to chlorenchymal tissues measured in longitudinal awn sections. Error bars, ±SD. BW ($n = 28$ cells, 3 awns), *ari-a.6*-BW ($n = 35$ cells, 3 awns). Welch's *t*-test was used for statistical analysis (**, $P \leq 0.01$). (g) Parenchymal cell length in the cell file adjacent to chlorenchymal tissues measured in transverse awn sections. Error bars, ±SD. BW ($n = 17$ cells of three awns), *ari-a.6*-BW ($n = 33$ cells of three awns). Welch's *t*-test was used for statistical analysis (**, $P \leq 0.01$). (h) Estimated cell numbers in BW and *ari-a.6*-BW awns. The values were obtained by dividing the average awn length by the average cell length and are expressed by the ratio to BW. (i) Amount of cell wall fractions and fraction weight (μg) per fresh weight (g), in awns and flag leaves of BW and *ari-a.6*-BW awns. Error bars, ±SD ($n = 3$ plants). Welch's *t*-test was used for statistical analysis (**, $P \leq 0.01$; *, $P \leq 0.05$; n.s., no significance).

are softer and crooked than those of BW. We considered that these differences might be due to alteration of the cell wall's components; thus, we analyzed the cell wall composition in 3-week-old awns after heading and flag leaves of *ari-a.6*-BW and BW. Compared with BW, *ari-a.6*-BW exhibited significant reductions in cellulose and hemicellulose in the awn cell walls, by 30% and 23%, respectively (Fig. 3i). In flag leaf, cellulose levels remained unchanged in *ari-a.6*-BW, whereas hemicellulose decreased, although not as markedly as in the awn (Fig. 3i). These findings suggest that SCA affects cell wall synthesis in the awns by affecting the biosynthesis of both cellulose and hemicellulose.

SCA encodes an EMF1 protein

To identify the gene causative of *sca*, we performed positional cloning using two genetic mapping populations derived from the crosses of *sca* (OUM206) with two long-awn cvs. Morex and Harrington. In the Morex × *sca* F_2 population (262 plants), *sca* was localized to a 0.6-cM interval between markers CA78986 and CA50813 on the 3HS arm, with distances of 0.4 and 0.2 cM from *sca*, respectively. Six markers cosegregated with *sca* (Supplementary Fig. S3). We planted another F_2 population (342 plants) from a cross between *sca* and Harrington, but only 80 recessive homozygous *sca* segregants were used for mapping (Supplementary Fig. S3). This cross was more recombinogenic in the *sca* candidate region because SC65023 was far from *sca* and mapped 1.9 cM distally. Although CA50813 was the proximal delimiting marker in the first population, this marker was not polymorphic in the second mapping population. Thus, *sca* was localized to a 2.5-cM interval between markers SC65023 and Bmac0067. Combining the two maps, we deduced that *sca* was located between SC65023 and CA50813. Then, through exploiting microsynteny between the barley 3HS arm and rice chromosome 1, we revealed that the *sca* candidate region corresponded to a 0.6-Mb physical interval in rice chromosome 1 containing 123 predicted genes in the Rice Genome Annotation Project (RGAP) database (Supplementary Fig. S3). In the Ensembl-Barley Morex V1 IBSCv2 genome database, this region includes 7962 barley genes spanning 521 Mb (*HORVU3Hr1G032410* to *HORVU3Hr1G112810*).

To further narrow down the candidate genes for *sca*, we conducted the deletion mapping on a panel of 27 independently induced *ari-a* mutants to detect small chromosomal deletions including the *sca* locus (Fig. 2a–d). For the deletion mapping, we used primers specifically designed to amplify gene regions among the barley homologs of 123 rice genes. Deletion mapping detected two chromosomal deletion mutants, namely, *ari-a.162* and *ari-a.279*, which both showed deletions encompassing *HORVU3Hr1G052490* to *HORVU3Hr1G052580* (866 kb; Supplementary Table S2). Of the 10 genes located within this interval, seven were confirmed to be deleted in both mutants (Fig. 2d, Supplementary Table S2). We sequenced two of the 10 candidate genes, *HORVU3Hr1G052490* and *HORVU3Hr1G052570* in wild-type parental cultivars (Bonus, Foma, and Kristina) and their corresponding mutants (*ari-a.6* and *ari-a.7*, *ari-a.118* and *ari-a.121*, and *ari-a.273* and *ari-a.277*, respectively). No mutations were detected in the coding regions (CDS, 1545 bp) of *HORVU3Hr1G052490* (syn. *HORVU.MOREX.r3.3HG0248990*), a homolog of the rice gene *LOC_Os01g12940* (syn. *Os01g0229800*). Sequencing of the coding regions (CDS, 3744 bp) of *HORVU3Hr1G052570* (syn. *HORVU.MOREX.r3.3HG0248910*), an ortholog of the rice gene *LOC_Os01g12890* (syn. *Os01g0229300*), detected various mutations in 21 mutants across the *ari-a* panel (Fig. 2e, Supplementary Table S3). Among the mutants, 16 mutants involve nonsense mutations and five involve frameshift mutations, resulting in truncated proteins (Fig. 2e, Supplementary Table S3) and thus presumably protein dysfunction. However, no mutation was identified in the sequenced CDS region in four mutants (Supplementary Table S3). We also found that the *sca* mutant has a 4-base deletion at an exon–intron junction in *HORVU.MOREX.r3.3HG0248910*, which was presumed to cause abnormal splicing, resulting in premature termination at that site (Fig. 2e, f, Supplementary Table S3). This gene, consisting of six exons and five introns, encodes a protein of 1247 amino acids with a molecular weight of 137.7 kDa. *HORVU.MOREX.r3.3HG0248910* is an ortholog of *EMF1* in *Arabidopsis thaliana* and rice. We further found a missense mutation in the short-awn mutant KM8 induced through γ-ray irradiation from Kanto Nijo 29 (Fig. 2e, Supplementary Table S3).

Using RNA sequencing (RNA-seq) mapped reads, candidacy of the remaining five genes (*HORVU3Hr1G052500*, *HORVU3Hr1G052510*, *HORVU3Hr1G052530*, *HORVU3Hr1G052540*, and *HORVU3Hr1G052560*) was excluded because these genes had no mutations in the CDS among these transcripts in BW, *ari-a.6*-BW, and *sca*-BW relative to the reference Morex genome. Transcripts of the remaining three genes in the candidate interval (*HORVU3Hr1G052520*, *HORVU3Hr1G052550*, *and HORVU3Hr1G052580*) were undetected.

These results collectively suggest that *HORVU.MOREX.r3.3HG0248910* is *SCA*.

Natural variation in *SCA* contributes to the diversity of barley awn length

Wild barley (*H. vulgare* subsp. *spontaneum*) OUH602 possesses slightly shorter awns than long-awn cv. Harrington and was reported to carry a quantative trait locus (QTL), AL4 on chromosome 3H, which shortens awns (Gyenis et al. 2007). Therefore, we sequenced the *SCA* gene in OUH602 and Harrington. Compared with the reference cv. Morex, two single-nucleotide polymorphisms resulting in missense mutations were found in the *SCA* coding region of OUH602 (Fig. 2e, Supplementary Table S3). To confirm whether this QTL corresponds to the *SCA* locus, we studied BC_1F_2 plants from crosses between OUH602 and Harrington. Progeny with the *SCA* region harboring the allele of OUH602 type exhibited shorter awns, averaging 73% of the length observed in the Harrington type (Fig. 1c, Supplementary Fig. S4). This suggests that the short-awn phenotype in wild barley OUH602 is caused by such amino acid substitutions in the SCA protein.

SCA is ubiquitously expressed and localized to the nucleus

In *Arabidopsis*, EMF1 is a plant-specific nuclear protein that represses transcription through interacting with PRC (Calonje et al. 2008). The SCA protein shares approximately 40% and 55% amino acid sequence similarity with EMF1 in *Arabidopsis* and rice, respectively, and all three proteins possess predicted nuclear localization signals and the LXXLL motif involved in protein interaction with nuclear receptors (Fig. 4a, Supplementary Fig. S5; Aubert et al. 2001; Heery et al. 1997). Five other conserved regions in EMF1 orthologous proteins were also found in SCA protein (Supplementary Fig. S5; Calonje et al. 2008).

To understand the biological function of SCA, we expressed an SCA–GFP fusion protein in tobacco leaf cells. Fluorescence signals of SCA–GFP were exclusively observed in the nucleus with mScarlet-I-fused histone H2B as a nuclear marker (Fig. 4b), indicating that SCA functions as a nuclear protein, consistent with the findings for *Arabidopsis* and rice EMF1 proteins (Calonje et al. 2008, Yan et al. 2015, Zheng et al. 2015). We also analyzed the expression pattern of *SCA* across different barley tissues and found that it is ubiquitously expressed, with relatively high levels in awns and leaves (Fig. 4c, d). The ubiquitous expression of *SCA* is consistent with the findings for *EMF1* expression in *Arabidopsis* and rice (Aubert et al. 2001, Yan et al. 2015, Zheng et al. 2015). In *Arabidopsis*, EMF1 represses its own expression through H3K27me3 repressive histone deposition (Kim et al. 2012). To explore whether this autoregulation also occurs in barley, we compared *SCA* expression in BW and two mutant NILs, finding that *SCA* expression was significantly lower in BW (Fig. 4e). These findings suggest that SCA, similar to EMF1 in *Arabidopsis* and rice, is a nuclear protein involved in transcriptional repression.

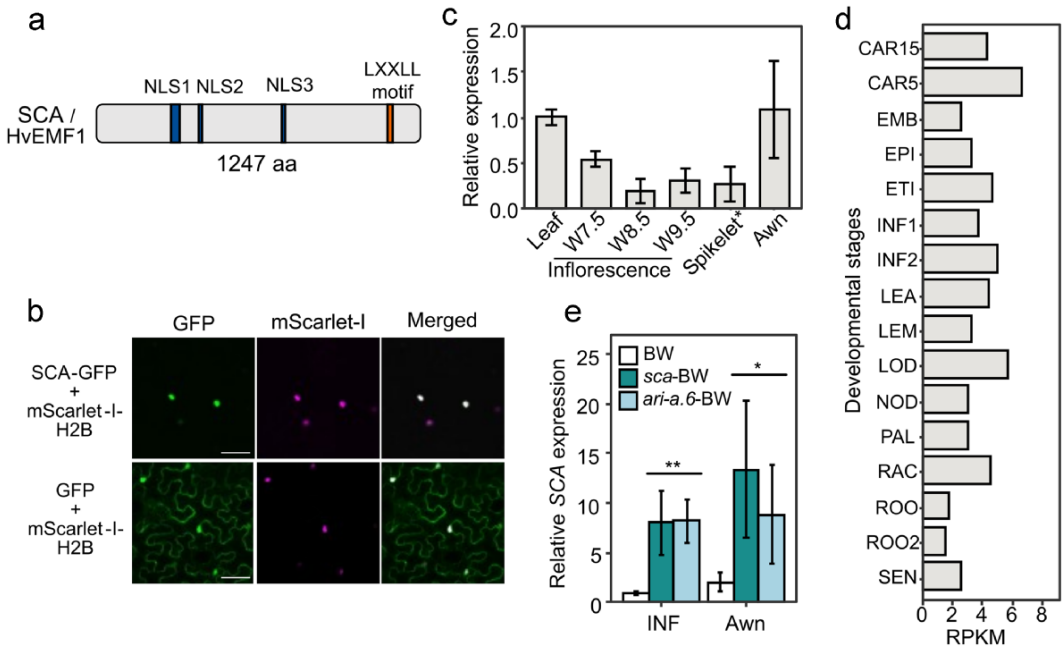

Figure 4. Subcellular localization and expression pattern of SCA. (a) Schematic representation of SCA protein. Nuclear localization signals (NLSs) and LXXLL motif are represented by colored boxes. (b) Subcellular localization of SCA–GFP and GFP protein in agroinfiltrated leaves of *Nicotiana benthamiana*. Bar = 50 μm. SCA–GFP protein (green) and the nuclear marker mScarlet-I-H2B (magenta) were localized in the nucleus, and GFP protein was localized in the cytoplasm and nucleus. (c) The relative expression of *SCA* in wild-type barley (BW) tissues was determined using quantitative RT-PCR. Inflorescences at Waddington scale W7.5, W8.5, and W9.5, spikelet* (spikelets at W9.5 excluding awns), awns harvested from spikelets at W9.5, and flag leaves were analyzed. *ACTIN* (*HORVU.MOREX.r3.1HG0003140*) was used as an internal control. Error bars, ±SD ($n = 3$ plants). (d) Tissue-specific expression pattern of *SCA*/*HORVU.MOREX.r3.3HG0248910* in Morex quantified as reads per kilobase of exon per million mapped reads (RPKM) values. These values were obtained from the barley expression database (BarleyExpDB). CAR15, Grain (15 days postanthesis, 15DPA); CAR5, grain (5 DPA); EMB, embryo (germinating); EPI, epidermis (4 weeks); ETI, etiolated (10-day seedlings); INF1, inflorescence (0.5 cm); INF2, inflorescence (1–1.5 cm); LEA, shoot (10 cm seedlings); LEM, lemma (6 weeks postanthesis, 6 weeks pa); LOD, lodicule (6 weeks pa); NOD, tillers (3rd internode); PAL, palea (6 weeks pa); RAC, rachis (5 weeks pa); ROO, root (10 cm seedlings); ROO2, root (4 week seedlings); SEN, senescing leaf (2 months). (e) The expression levels of *SCA* were compared among BW, *sca*-BW and *ari-a.6*-BW in INF (inflorescences at W7.5) and awns harvested from spikelets (W9.5). Error bars, ±SD ($n = 3$ plants). *ACTIN* (*HORVU.MOREX.r3.1HG0003140*) was used as an internal control. Statistical analysis was performed using Student's *t*-test (**, $P \leq 0.01$; *, $P \leq 0.05$).

SCA affects the expression of awn-related genes

We performed RNA-seq analysis on inflorescences at stage W7.5 and fully elongated awns at the heading stage (Waddington et al. 1983), identifying differentially expressed genes (DEGs) between the mutant NILs and BW (Fig. 5a, b). In inflorescences, *ari-a.6*-BW had 48 upregulated and 373 downregulated DEGs, whereas the corresponding numbers in *sca*-BW were 71 and 551, respectively, with 10 upregulated and 62 downregulated DEGs being shared between the two mutant NILs (Fig. 5a, b). In awns, *ari-a.6*-BW had 386 upregulated and 1119 downregulated DEGs, whereas the corresponding numbers in *sca*-BW were 1733 and 3193, respectively. The two mutant NILs shared 277 upregulated (72% in *ari-a.6*-BW) and 544 downregulated DEGs (49% in *ari-a.6*-BW; Fig. 5a, b). More DEGs were observed in *sca*-BW than in *ari-a.6*-BW. This difference was clearer in the awns, suggesting the severe effects of the *SCA* mutation on awn elongation. Additionally, *SCA* was among the three upregulated DEGs in both mutant NILs in the inflorescence and awn (Fig. 5a). The upregulation of *SCA* is consistent with the RT-qPCR results (Fig. 4e). In *sca*-BW, RNA-seq mapped reads confirmed that the 4-bp deletion spanning the exon–intron junction alters the splicing pattern of *SCA* transcript, leading to the immediate appearance of a premature stop codon (Supplementary Fig. S6).

To determine the SCA's role in awn development, we assessed the changes in awn-related gene expression in the mutant NILs (Fig. 5c). The barley genes *Lks2*, *HvMADS1*, and *HvAP2*; the rice genes *RAE1*, *RAE2*, *RAE3*, *LABA1*, and *DL*; and the wheat gene *WFZP* are involved in promoting awn elongation. The orthologs of *RAE2* and wheat awn inhibitor *B1* were not detected in barley by our homology search. Although the *WFZP* ortholog was found in barley, it was not expressed. *Lks2*, *HvRAE1*, *HvRAE3*, and *HvLABA1* were downregulated in *sca*-BW awns. *HvMADS1* was downregulated only in *sca*-BW inflorescences. Ectopic expression of *BKn3* is known to disrupt normal awn development in barley (Müller et al. 1995), and its ortholog has been revealed to be directly repressed by EMF1 in *Arabidopsis* (Kim et al. 2012). Our results showed that *BKn3*

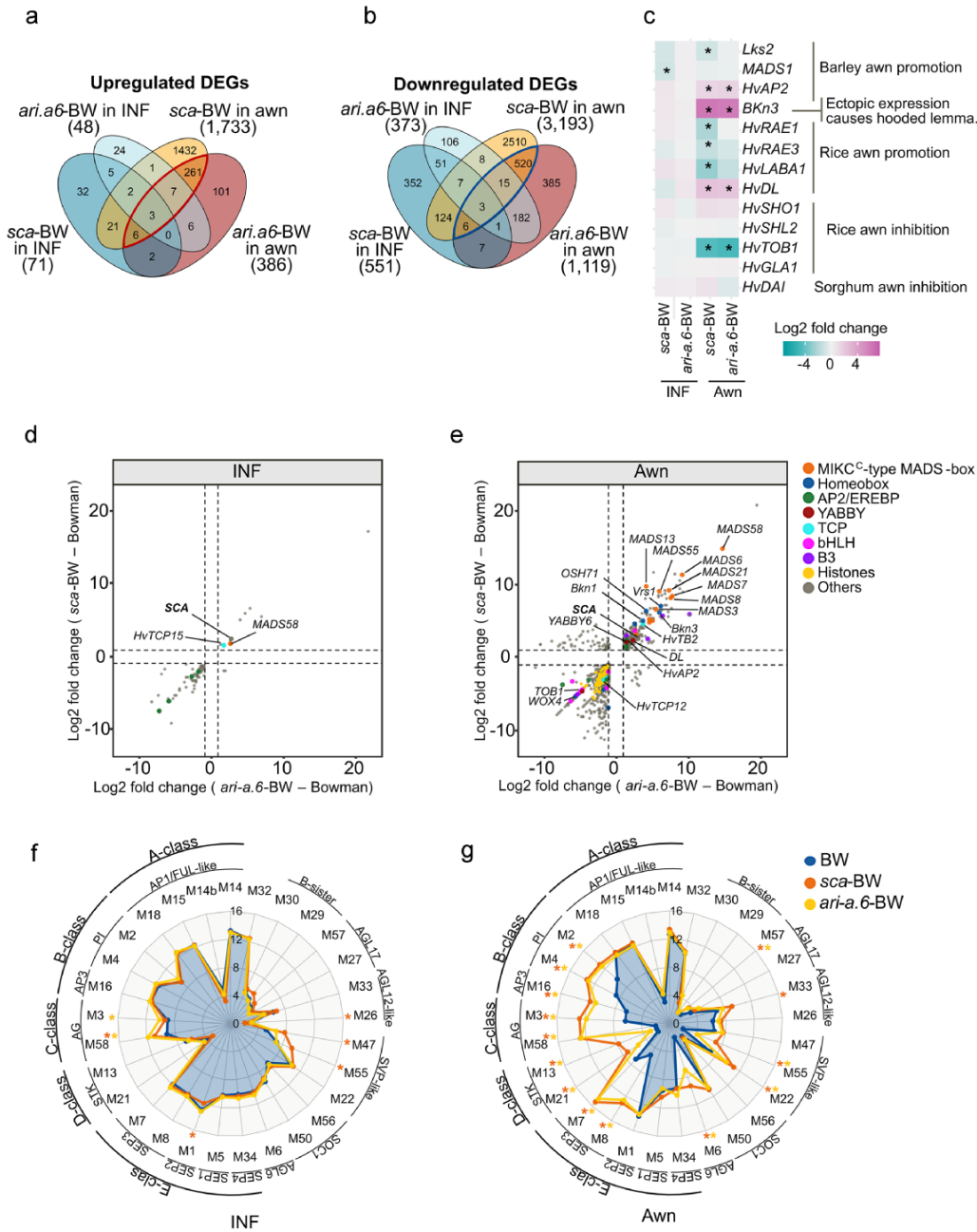

Figure 5. Impairment of SCA disrupts the expression of awn-related genes and homeotic genes including the MADS-box family. Venn diagram showing the number of DEGs upregulated [Log2 fold change > 1, FDR < 0.05] (a) and downregulated [Log2 fold change < −1, FDR < 0.05] (refer to Supplementary Data S1) (b) in *sca*-BW and *ari-a.6*-BW in the INF (inflorescence at W7.5) and awn compared with the levels in BW. The common DEGs in the awn are enclosed by red and blue lines. (c) Heatmaps showing the differential expression (Log2 fold change) in *sca*-BW and *ari-a.6*-BW compared with BW of genes related to awn development (refer to Supplementary Data S2). Asterisks (*) indicate DEGs [|Log2 fold change| > 1, FDR < 0.05] in mutant NILs compared with that in BW. *SHO1: SHORT SHOOT ORGANIZATION 1; SHL2: SHOOTLESS* 2. Scatter plot illustrating a comparison between *sca*-BW and BW on the *x*-axis, and *ari-a.6*-BW and BW on the *y*-axis in INF (inflorescence at W7.5) (d) and in awn (e). The gray points represent common DEGs, while the other colored points represent MIKC^C-type MADS-box family; Homeobox including KNOX1 genes, HD-ZIP family, and WOX gene; APETALA2/ethylene-responsive element binding protein (*AP2/EREBP*) family; YABBY family; TEOSINTE BRANCHED1, CYCLOIDEA, and PROLIFERATING CELL FACTOR (TCP) family; and bHLH family, B3 domain–containing genes and histones (refer to Supplementary Data S3). The dashed axes indicate the|Log2 fold change| = 1 in expression of DEGs in the two comparisons. Radar chart displaying expression levels of MIKC^C-type MADS-box genes in BW (blue line), *sca*-BW (orange line), and *ari-a.6*-BW (yellow line). Expression levels are quantified as log2 (CPM + 4) for the INF (inflorescence at W7.5) (f) and awn (g). "MADS" is abbreviated as "M," and the corresponding class is indicated outside the gene names (refer to Supplementary Data S4). Orange asterisks indicate DEGs in *sca*-BW compared with BW, while yellow asterisks represent DEGs in *ari-a.6*-BW compared with BW. Blue shading in the chart represents the expression profile of MIKC^C-type MADS-box genes in BW.

was upregulated in both mutant NIL awns (Fig. 5c, e). These changes in expression may inhibit awn development in mutant NILs. Interestingly, *HvAP2* and *HvDL* were upregulated in both mutant NIL awns (Fig. 5c, e). The repression of *HvDL* by SCA is consistent with the regulation of its orthologs, namely, repression of *CRC* in *Arabidopsis* and *DL* in rice by EMF1 (Kim et al. 2012, Yan et al. 2015, Zheng et al. 2015). Conversely, the YABBY gene *HvTOB1*, which suppresses awn development in rice, was downregulated in both mutant NIL awns (Fig. 5c, e). These changes in expression in *HvDL*, *HvTOB1*, and *HvAP2* do not align with the short-awn phenotype observed in the mutant NILs; however, they suggest a more complex regulatory role for SCA, potentially involving feedback loops or other antagonistic pathways that modulate awn development.

Loss of SCA impairs the repression of MIKC^C-type MADS-box family genes in awn

In addition to the genes previously known to be involved in awn development, numerous genes encoding TFs were found as DEGs overlapping between *sca*-BW and *ari-a.6*-BW (Fig. 5d, e). In the inflorescence, *HvMADS58* (orthologous to *AG* in *Arabidopsis*) and the Class II TCP family gene *HvTCP15* were upregulated and AP2/EREBP superfamily members were downregulated (Fig. 5d). In the awns, many MADS-box genes, KNOX1 genes (e.g. *BKn1* and the ortholog of rice homeobox gene *OSH71*), YABBY genes (e.g. *YABBY6*), HOMEODOMAIN-leucine zipper (HD-ZIP) genes (e.g. *Six-rowed spike 1*(*Vrs1*)/*HvHOX1* and *HvHOX2*), and the Class II TCP family gene barley *TEOSINTE BRANCHED 2* (*HvTB2*) were upregulated (Fig. 5e). Conversely, downregulated TFs in the mutant NIL awns included Class II TCP family gene *HvTCP12* and *WUSCHEL-RELATED HOMEOBOX4* (*WOX4*), which regulates cell cycle–related genes (Fig. 5e; Yasui et al. 2018). Additionally, bHLH family genes, B3 domain–containing TF genes, and AP2/EREBP superfamily members were identified as DEGs in the awns of both mutant NILs (Fig. 5e).

Among the TFs identified as common DEGs, MIKC^C-type MADS-box genes were highly expressed in the awns of both mutant NILs (Fig. 5e, g). MIKC^C-type MADS-box genes form the core of the ABCDE model, which explains how five classes of homeotic genes define floral organ identity (Coen and Meyerowitz 1991, Weigel and Meyerowitz 1994, Becker and Theißen 2003). In grasses, the ABCDE model, originally established in core dicots, is adapted such that A-class genes specify the lemma and palea (Whorl 1), A- and B-class genes identify lodicules (Whorl 2), B- and C-class genes regulate stamens (Whorl 3), and C-class genes form the pistil (Whorl 4). D-Class genes, along with C-class ones, specify ovary identity, whereas E-class genes determine all floral organs and regulate meristem determinacy (Ciaffi et al. 2011, Yoshida and Nagato 2011, Murai 2013, Kuijer et al. 2021). With the exception of the A-class gene *AP2* and the C-class gene *DL* in rice, all ABCDE model genes are MADS-box genes (Nagasawa et al. 2003, Yamaguchi et al. 2004, Causier et al. 2010).

In barley, the loss of SCA primarily results in shortened awns, with no major morphological changes observed in other floral organs (Supplementary Fig. S7). In contrast, the rice *emf1* mutants, *deformed floral organ 1* (*dfo1*) in the indica variety and *curved chimeric palea 1* (*ccp1*) in the japonica variety, exhibit a shrunken and carpeloid palea, with *dfo1* also showing elongated awns, inner organ abnormalities such as stamen and lodicule deformities or losses, and an increase in pistil number (Yan et al. 2015, Zheng et al. 2015). These morphological changes in rice *emf1* mutants are thought to result from the ectopic expression of C-class genes caused by the loss of EMF1 function.

The loss of SCA in barley leads to the upregulation of C-class genes (*HvMADS58* and *HvMADS3*), similar to what is observed in rice (Fig. 5d–g). Additionally, in barley, D-class genes (*HvMADS13* and *HvMADS21*), as well as B-class genes (*HvMADS2*, *HvMADS4*, and *HvMADS16*), are upregulated in the awns of both mutant NILs (Fig. 5e, g). Among the E-class genes, SEP3-like genes (*HvMADS7* and *HvMADS8*), which function in the inner floral organs, are also upregulated (Fig. 5e, g). The AGL6-like gene *HvMADS6*, which functions similar to E-class genes but is not expressed in the lemma (Li et al. 2010, Sun et al. 2024), was ectopically expressed in the awns of both mutant NILs (Fig. 5e, g). A-Class (AP1/FUL-like) gene expression remains unchanged (Fig. 5f, g). Genes outside the ABCDE model, such as SVP-like genes (*HvMADS22* and *HvMADS55*), the AGL12-like gene (*HvMADS33*), and the AGL17 gene (*HvMADS57*), are ectopically expressed in the awns of barley mutant NILs (Fig. 5e, g). In the inflorescence, *HvMADS58* is highly expressed in both mutant NILs, while SEP-like gene *HvMADS1* and AGL12-like gene *HvMADS26* are slightly downregulated in *sca*-BW (Fig. 5d, f).

Notably, in rice *emf1* mutant, while C- and D-class genes are upregulated similar to barley mutant NILs, B- and A-class genes are notably downregulated (Yan et al. 2015, Zheng et al. 2015). In contrast to rice *emf1* mutant, the increased expression of B-class genes with C-class genes in barley mutant NILs might have preserved stamen and lodicule identity. Additionally, the stable expression of A-class genes, which regulate lemma and palea, might prevent the palea deformities in barley mutant NILs.

SCA promotes the expression of genes related to cell proliferation, cell elongation, and cell wall synthesis in awn

To explore how SCA affects cell proliferation, cell elongation, and cell wall formation during awn development, we performed Gene Ontology (GO) analysis (Fig. 6a, b, Supplementary Fig. S8A–C). Downregulated DEGs overlapping in both mutant NILs were enriched in terms related to DNA replication, cell division, auxin response, and cell wall biogenesis (Fig. 6a), while upregulated DEGs were enriched in terms linked to transcriptional regulation, signal transduction, and auxin transport (Fig. 6b, Supplementary Fig. S8B). Among the DEGs involved in cell proliferation are the G_1/S-specific cyclin *CYCD1;1* and core components of the DNA replication machinery such as *MINICHROMOSOME MAINTENANCEs* (*MCMs*) and *PROLIFERATING CELL*

NUCLEAR ANTIGEN 1 (*PCNA1*), which is expressed during the S phase (Fig. 6c, Supplementary Fig. S8C). Additionally, histones, including *HISTONE H4*, a marker of active cell division, are also downregulated (Supplementary Fig. S8A, C, and D). These findings suggest a decrease in S-phase cells in both mutant NILs, indicating that SCA may be involved in cell cycle progression, thereby accelerating cell proliferation in awns. Meanwhile, in rice, awn elongation is associated with cytokinin-mediated cell proliferation, involving genes such as *LABA1* and *RAE2*, which activate cytokinin. In the awns of mutant NILs, the expression of *HvLABA1* was downregulated (Fig. 5c), and furthermore, the expression of cytokinin-related genes varied, with *CYTOKININ OXIDASE/DEHYDROGENASE 2* (*CKX2*), an enzyme that degrades cytokinin, upregulated (Fig. 6d). These findings suggest that reduced cytokinin levels in the mutant NILs may cause decreased cell proliferation and result in reduced cell number in the awn. Additionally, the expression of auxin-related genes, including the auxin-responsive *AUXIN/INDOLE 3-ACETIC ACID* (*Aux/IAAs*), *GRETCHEN HAGEN 3* (*GH3*), and *SMALL AUXIN UP RNA* (*SAURs*) (Hagen and Guilfoyle 2002), and genes related to auxin distribution such as auxin influx carriers *AUXIN1/LIKE AUX1* (*AUX/LAX*), the auxin transporter *PIN-FORMED* (*PIN1B*), PIN1 localization regulator *PATELLINs* (*PATLs*), and *WALLS ARE THIN 1* (*WAT1*), was reduced in the awns of both mutant NILs (Fig. 6d). WAT1 is involved in auxin homeostasis and the formation of secondary cell walls in *Arabidopsis* (Ranocha et al. 2013). The changes in expression of auxin-related genes in the awns of both mutant NILs suggest that SCA influences the auxin response and auxin transport homeostasis, contributing to cell elongation in the awns.

Regarding synthesis of the cell wall, the expression of genes involved in xylan (glucuronoarabinoxylan) biosynthesis, such as *IRREGULAR XYLEM 9/10* (*IRX9/10*), *GLUCURONIC ACID SUBSTITUTION OF XYLAN 1* (*GUX1*), and *XYLOSYL ARABINOSYL SUBSTITUTION OF XYLAN 1* (*XAX1*), as well as genes crucial for nucleotide sugar metabolism, *UDP–GLUCOSE DEHYDROGENASE 2/3* (*UGD2/3*), and *UDP-XYLOSE SYNTHASE 1/3* (*UXS1/3*), was reduced in the awns of *sca*-BW (Fig. 6e). Xylan is a main component of hemicellulose in grass plants. Additionally, *COBRA*-Like (*COBL*), involved in cellulose deposition, was also downregulated in *sca*-BW awns (Fig. 6e). In *ari-a.6*-BW awns, the expression of *UGD3* and *HvCOBL7* was also reduced (Fig. 6e). The downregulation of these genes due to SCA dysfunction could lead to significant decreases in hemicellulose and cellulose observed in *ari-a.6*-BW awns (Fig. 3i). Furthermore, the genes important in secondary cell wall synthesis, such as *BRITTLE CULM 3* (*BC3*)/ *DYNAMIN-RELATED PROTEIN 2B* (*DRP2B*) and *BC15*, were downregulated in the awns of *sca*-BW (Fig. 6e). Similarly, *LACCASEs* (*LACs*), which are essential for the biosynthesis of lignin, were downregulated in both mutant NIL awns (Fig. 6e). These results indicate that SCA may facilitate secondary cell wall synthesis by promoting the expression of these genes.

SCA is required for gene repression via histone H3K27 trimethylation

The repression of *AG* and its rice ortholog *OsMADS58* by EMF1 in *Arabidopsis* and rice involves histone H3K27 trimethylation, functioning with the PRC2 (Calonje et al. 2008, Kim et al. 2010, 2012, Yan et al. 2015, Zheng et al. 2015). In barley, similar to the findings in *Arabidopsis* and rice, the *AG* ortholog *HvMADS58* is overexpressed due to SCA dysfunction (Fig. 5d–g). We investigated whether SCA-mediated gene repression in barley is associated with H3K27me3 deposition by performing chromatin immunoprecipitation (ChIP)-qPCR analysis in awns using a histone H3K27me3 antibody.

The awns of *ari-a.6*-BW and BW were used for ChIP analysis, as insufficient quantities of the *sca*-BW awns were yielded. The H3K27me3 deposition at the *HvMADS58* and *SCA* loci was reduced in *ari-a.6*-BW compared with the level in BW (Fig. 7a, b). These results indicate that SCA is involved in the accumulation of H3K27me3 in these loci. Meanwhile, no change in H3K27me3 deposition was observed at the *HvMADS3*, *HvMADS6*, and *HvMADS13* loci in *ari-a.6*-BW (Fig. 7b). These genes were highly expressed in mutant NIL awns, but were not upregulated in the inflorescence (Fig. 5d–g). These results suggest that the repression of *SCA* and *HvMADS58* by SCA is linked to the SCA-dependent accumulation of H3K27me3.

Discussion

Molecular cloning of the *SCA* gene

The short-awn mutants, *sca*, *ari-a*, and KM8, were independently induced from different original accessions (Kucera et al. 1975, Moriya and Takahashi 1980, Konishi et al. 1984, Druka et al. 2011). Among these mutants, we identified mutations or deletions in the *HORVU3Hr1G052570* (syn. *HORVU.MOREX.r3.3HG0248910*) gene, which encodes an EMF1 protein, in 25 mutants (Fig. 2e, f, Supplementary Table S3). We also demonstrated that *HORVU.MOREX.r3.3HG0248910* is ubiquitously expressed and involved in the H3K27me3 deposition of the *AG* ortholog *HvMADS58* (Figs. 4c, d, 5d–g, and 7b). These findings are consistent with the identified function of EMF1 in *Arabidopsis* and rice, strongly indicating that the *EMF1* ortholog *HORVU.MOREX.r3.3HG0248910* gene as *SCA* is responsible for the short-awn phenotype in *sca*, *ari-a*, and KM8.

An awn length QTL (AL4) was reported on the 3HS chromosome arm in the cross wild barley OUH602 × long-awn cv. Harrington cross, with OUH602 allele having an effect to reduce awn length (Gyenis et al. 2007). We detected nonsynonymous substitutions in the *sca* locus of OUH602 (Fig. 2e, Supplementary Table S3). Furthermore, phenotypic segregation of awn lengths in the Harrington × OUH602 BC_2F_2 generation selected by the *sca*-flanking markers in this study showed that the *SCA* locus coincides with this AL4 QTL of wild barley OUH602 allele (Fig. 1c, Supplementary Fig. S4). This study sequenced a limited

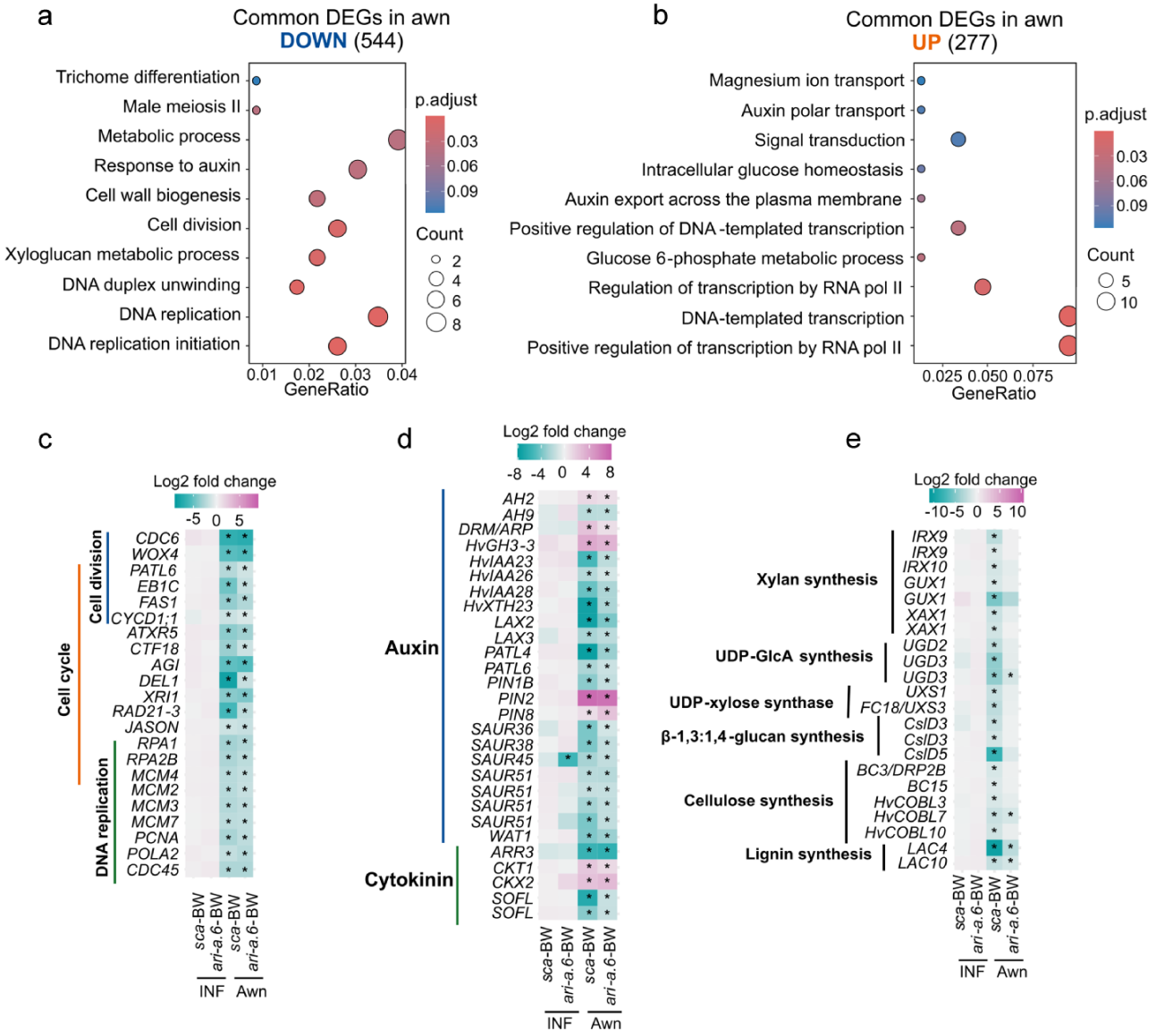

Figure 6. Dysfunction of SCA causes changes in the expression of genes related to cell proliferation, cell elongation, cell wall synthesis, and associated hormones in awn. Top enriched GO terms in biological processes among 544 downregulated DEGs (a) and 277 upregulated DEGs (b) common to *sca*-BW and *ari-a.6*-BW in the awn. Heatmaps showing the differential expression (Log2 fold change) of genes related to cell proliferation (c), cell wall (d), and hormones (e) in *sca*-BW and *ari-a.6*-BW compared with the levels in BW (refer to Supplementary Data S2). Asterisks (*) indicate DEGs in mutant NILs compared with that in BW.

number of wild and domesticated barley accessions, but at least two types of nonsynonymous substitutions were detected in the *sca* locus (Fig. 2e, Supplementary Table S3). Thus, the *sca* locus should be partly responsible for natural variation in awn lengths among intermediate- to long-awn accessions of barley. In sharp contrast, artificially induced *sca* mutants tested in this study all showed extremely short-awn phenotypes (Figs 1a, 2a–c). Those artificial mutations seem to affect functionally indispensable sites (Fig. 2e, Supplementary Table S3), and therefore, such severely short and thin awn mutants are likely to have reduced fitness in the wild.

SCA is involved in multiple pathways associated with awn development

We found that SCA facilitates awn elongation by promoting cell proliferation and cell elongation (Fig. 3f–h). This is further supported by our finding that, in the awn, loss of SCA function resulted in disrupted expression of genes linked to cytokinin-mediated cell proliferation and decreased expression of genes critical for cell cycle progression, suggesting a reduction in S-phase cells (Fig. 6c, d, Supplementary Fig.S8). Additionally, the loss of SCA function led to reduced expression of genes involved in auxin-mediated cell elongation (Fig. 6d).

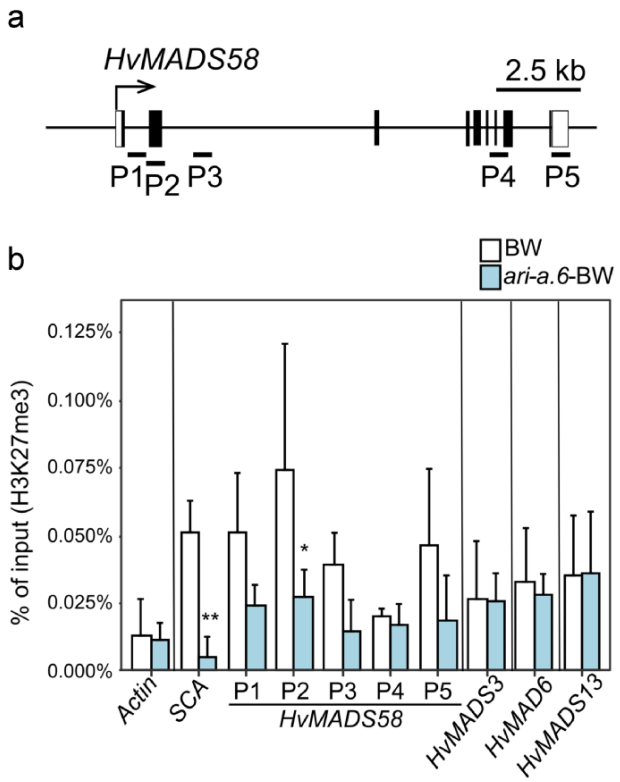

Figure 7. Dysfunction of SCA reduces histone H3K27me3 levels at specific loci. (a) Diagram illustrating the genomic region of *HvMADS58*. ChIP-qPCR was performed on five chromatin regions within *HvMADS58*, represented by P1–P5. The black boxes represent exons, and white boxes represent untranslated regions. (b) Histone H3K27me3 deposition at *SCA*, *HvMADS58*, *HvMADS3*, *HvMADS6*, and *HvMADS13* in BW and *ari-a.6*-BW awn by ChIP-qPCR analysis. The *ACTIN* locus (*HORVU.MOREX.r3.1HG0003140*) served as a negative control. The values were calculated using the percent of input. Error bars, ±SD. Biological replicates $n = 3$. Statistical analysis was performed using Student's *t*-test (**, $P \leq .01$; *, $P \leq .05$).

We also revealed that SCA participates in the accumulation of cell wall components, particularly hemicellulose and cellulose, in awns (Fig. 3i). SCA activates *LACs* for lignin synthesis in secondary cell wall formation and *COBL7* for cellulose deposition (Fig. 6e). More importantly, SCA regulates genes essential for producing major hemicellulose components in grass species. Specifically, SCA may contribute to xylan synthesis by upregulating *UGD3*, an enzyme in nucleotide sugar metabolism that converts UDP–glucose to UDP–glucuronic acid (Fig. 6e).

Our study also showed that SCA plays a role in regulating genes associated with awn development. We found that the loss of SCA function led to downregulation of the awn-promoting genes *Lks2*, *HvRAE1*, *HvRAE3*, and *HvLABA1* in the awn (Fig. 5c). However, since this effect was significant only in *sca*-BW with its severely shortened awns, these changes may reflect the short-awn phenotype rather than being a direct consequence of SCA dysfunction (Fig. 1). We discovered that SCA represses the expression of the KNOX1 gene *BKn3*, a barley ortholog of rice *OSH1*, in the awn (Fig. 5c, e). Ectopic expression of *BKn3* disrupts auxin transport by affecting the localization of PIN1, leading to the hooded phenotype, characterized by a loss of awn identity and reversed spikelet orientation (Müller et al. 1995, Richardson et al. 2016). In the awns of mutant NILs, the expression of *PINs* and auxin influx carrier *LAXs* was disrupted (Fig. 6d). These findings suggest that SCA could be involved in cell polarity and elongation in the awn through repressing *BKn3*. In addition, SCA represses the other KNOX1 genes *BKn1* and *HvOSH71* (Fig. 5e). SCA also regulates YABBY genes in ways that counter its role in promoting awn elongation, repressing the awn-promoting gene *HvDL*, and promoting the awn-suppressing gene *TOB1* (Fig. 5c, e). Furthermore, SCA represses barley *YABBY6* in the awns (Fig. 5e). Since YABBY and KNOX1 are known to cross-regulate and shape nodes and internodes (Tsuda et al. 2024), our findings suggest that SCA coordinates this YABBY–KNOX1 cross-regulation in the awn.

We also found that the *AG* ortholog *HvMADS58* is the only TF among the upregulated genes in the inflorescences and awns of the mutant NILs (Fig. 5d–g). *AG* genes in *Arabidopsis* and rice are primary targets of EMF1 (Calonje et al. 2008, Yan et al. 2015, Zheng et al. 2015). In rice, the overexpression of *OsMADS58* mimics EMF1 loss and the palea abnormalities caused by EMF1 deficiency are rescued by knocking down *OsMADS58*, indicating that EMF1 regulates palea identity by repressing *OsMADS58* (Yan et al. 2015, Zheng et al. 2015). Although the function of HvMADS58 in barley remains unclear, the role of SCA, which specifically affects awn development in barley spikelets, might reflect differences in the functional roles of MADS58 between barley and rice. As a hypothesis, SCA might influence awn development in barley through the repression of *HvMADS58*. However, the exact mechanisms through which SCA is involved in awn development remain unclear, and further research is needed to identify the genes directly regulated by SCA and to characterize the contributions of *HvMADS58*, *BKn3*, and other SCA-regulated genes to awn development.

Distinct effects of EMF1 in floral organ development between rice and barley

The effects of EMF1 on floral development differ significantly between rice and barley. In rice, the loss of OsEMF1 can lead to various abnormal morphological features of floral organs, such as elongated awns, palea-to-carpeloid transformation, partial transformation of lodicules into pistil-like structures, a lack of stamens, and multiple pistils (Yan et al. 2015, Zheng et al. 2015). In contrast, the loss of SCA in barley primarily results in shortened awns (Fig. 1d, Supplementary Fig. S2C), while having no significant impact on other floral organs (Supplementary Fig. S7). These phenotypic differences may arise from variations in the regulation of MADS-box genes within the ABCDE model of floral development.

In barley, C- and D-class MADS-box genes are ectopically expressed in mutant NILs (Fig. 5e, g), similar to what is observed in rice upon the disruption of EMF1 (Yan et al. 2015, Zheng et al. 2015). However, B-class genes show opposite trends in barley

and rice: they are upregulated in barley but downregulated in rice upon the loss of function of EMF1 (Fig. 5e, g; Zheng et al. 2015). In rice, the combined effect of C-class gene upregulation and B-class gene downregulation may affect the identity and number of lodicules and stamens, leading to pistil-like features. In contrast, the upregulation of B-class genes in barley, as well as C-class genes, might still maintain their balance and, as a result, prevent the loss of stamen identity in the mutant NILs. In the ABCDE model, A- and C-class genes are antagonistic; this relationship is also conserved in rice, where reduced A-class gene expression results from the overexpression of C-class genes (Yamaguchi et al. 2004). However, this antagonistic regulatory pattern is not found in barley (Kuijer et al. 2021, Chen et al. 2023). Consistent with this, when C-class genes are overexpressed due to *EMF1* mutation, the expression of A-class genes remains unchanged in barley (Fig. 5d–g), while it decreases in rice (Zheng et al. 2015). The differences in regulation of B-class genes by EMF1 and the relationship between A- and C-class genes may contribute to the distinct morphological outcomes observed in these species.

An intriguing difference in spikelet morphology between barley and rice *emf1* mutants is that the loss of EMF1 function leads to awn shortening in barley, while in indica rice, it results in awn elongation (Yan et al. 2015, Zheng et al. 2015). It has been reported that *DL* is upregulated in rice *emf1* mutants. DL is involved in awn elongation in the awned indica strain Kasalath but requires the expression of *OsETTEN2* (*OsETT2*) in the awn primordium to function (Toriba and Hirano 2014). In japonica rice, *OsETT2* is not expressed in the awn primordium, and thus DL cannot promote awn elongation. This explains why *DL* upregulation is observed in both indica and japonica *emf1* mutants, yet awn elongation occurs only in indica. Therefore, awn elongation in rice *emf1* mutants could be linked to the *DL* gene regulation pathway. In barley, HvDL also plays a role in awn elongation (Zhang et al. 2024). However, we showed that despite the upregulation of *HvDL* in loss of EMF1 function in barley (Fig. 5c, e), the awns notably shorten. This fact can be explained by the fact that other downstream awn-related genes regulated by SCA, which may not exist or function in rice, have a significant influence in barley.

To clarify the differences in EMF1's impact on the development of floral organs including awn between rice and barley, it is necessary to understand in more detail the regulatory differences in the genes involved in the morphology of floral organs that are controlled by EMF1.

Potential epigenetic regulatory mechanisms by SCA

Our results suggested that SCA represses *HvMADS58* and *SCA* itself through SCA-dependent H3K27me3 deposition (Figs 4e, 5d–g, and 7b), consistent with the findings for *Arabidopsis* and rice EMF1. The molecular mechanism associated with the epigenetic regulation of EMF1 has been reported in *Arabidopsis*. AtEMF1 protein interacts with the PRC2 core component MSI1 and the RING-finger homologs AtBMI1A/B and AtRING1A/B, which are part of the plant PRC1-like complex in *Arabidopsis* (Calonje et al. 2008, Kim et al. 2012, Yan et al. 2015, Zheng et al. 2015). EMF1 also directly interacts with H3K27me3 readers LHP1 in the PRC1-like complex, SHL, and EBS (Wang et al. 2014, Yin et al. 2021). A recent study has shown that, although EMF1 does not participate in PRC1-mediated H2A ubiquitination (H2Aub), EMF1 collaborates with PRC2 to repress genes involved in development and plays an important role downstream of H2Aub by reducing chromatin accessibility, which, in turn, contributes to an increased level of H3K27me3 (Yin et al. 2021). In rice, OsEMF1 protein interacts with the PRC2 components OsMSI1 and OsiEZ1 and the H3K27me3 readers OsSHL and OsEBS, but not with OsLHP1. The nature of the interaction between the OsEMF1 and OsRING proteins is still unclear, with conflicting results having been reported (Yan et al. 2015, Zheng et al. 2015). In any case, OsEMF1 mediates H3K27me3 deposition via the PcG mechanism. Based on these functions of EMF1 in rice and *Arabidopsis*, it is plausible that SCA facilitates the access of PRC2 to target genes for the accumulation of H3K27me3. Although the understanding of the involvement of SCA in H3K27me3 deposition in barley development and morphogenesis including awn development is still limited, SCA might employ this epigenetic mechanism to precisely repress genes that must remain silenced, ensuring proper awn development.

It has also been shown that EMF1 in *Arabidopsis* and rice regulates gene expression independent of H3K27me3, such as in vegetative development, by upregulating photosynthesis and chloroplast genes through suppression of the m5C RNA methyltransferase *TRM4B* via H3K4me3 in *Arabidopsis* (Zhang et al. 2023), and in brassinosteroid signaling by activating *OsBRI1* expression in rice (Liu et al. 2018). SCA is crucial not only for awn development but also for other agronomic traits such as plant height and grain yield. These effects of SCA on plant development and architecture might involve diverse regulatory pathways, including mechanisms beyond H3K27me3-mediated gene repression. It is crucial to unravel the molecular mechanisms of SCA-mediated awn development and its agronomic effects in order to advance barley breeding efforts and unlock barley's full potential.

Materials and Methods

Plant materials and growth conditions

For genetic mapping of the *sca* locus, F_2 plants derived from the crosses of *sca* mutant (OUM206, six rows) with two long-awn cvs. Morex (six rows) and Harrington (two rows) were used. For deletion mapping, the *sca* mutant (OUM206) and wild-type cv. Akashinriki, as well as 27 *ari-a* mutants induced in cv. Bonus, Foma, and Kristina, were used. To confirm variations at the *sca* locus, short-awn mutant KM8 induced by γ-ray irradiation from Kanto Nijo 29 was also used. Wild barley accession OUH602 and cv. Harrington were used to test whether the *sca* allele corresponds to the QTL AL4. For genetic analysis, long-awn cv. BW and its NILs, *sca*-BW and *ari-a.6*-BW, were employed.

To measure agronomic traits of BW, *sca*-BW, and *ari-a.6*-BW, the 2019 and the 2020 batches were sown in seedbeds and transplanted to the field at the Institute of Plant Science and Resources, Okayama University in Kurashiki, Japan, at 7 weeks, with harvesting ~30 weeks after sowing. After drying for one week and treatment of pest control at -20°C for two weeks, the agronomic

traits were measured. Awn lengths were measured at three positions: the fourth spikelet from the top, the middle spikelet, and the fourth spikelet from the bottom. The number of days from seed sowing to the emergence of half of the spike was considered as the number of days to heading. For phenotyping, Akashinriki and OUM206 were grown in a greenhouse. To measure cell wall polysaccharides, BW and *ari-a.6*-BW were grown in the greenhouse. For genetic mapping, OUM206, cvs. Morex, and Harrington, along with their F_2 populations, were grown in the field. An allelism test was performed by intercrossing *ari-a.6*-BW and *sca*-BW, and F_1 awn phenotypes were visually confirmed ~3 weeks after flowering in a controlled environment at 18°C–25°C under natural light. All plants used for deletion mapping, RT-qPCR, and RNA-seq analysis were grown in the greenhouse. To test whether the *sca* allele corresponds to QTL AL4, a Harrington × OUH602 BC_1F_2 population was grown in the greenhouse. For ChIP analysis and observation of spikelets and awns, BW and mutant NILs were grown in the controlled environment at 18°C–25°C under natural light. For agroinfiltration, *Nicotiana benthamiana* plants were grown under 12-h light/12-h dark at 24°C until they developed six leaves, with the youngest leaves measuring >1 cm in length.

Measurement of polysaccharides constituting cell walls

Awn and flag leaf samples were collected from three individual plants of BW and *ari-a.6*-BW at 3 weeks after heading. The analysis was conducted in accordance with a previous report (Kutsuno et al. 2023). The collected samples were frozen in liquid nitrogen, ground with a mortar and pestle while still frozen, then thawed, and mixed with water. The samples were further ground with a mortar and pestle and subsequently centrifuged at 21 500*g* for 5 min at 4°C. The resulting supernatant was used as the soluble fraction. The precipitate was then suspended in 800 μl of 80% ethanol and boiled for 2 min. After another round of centrifugation under the same conditions as described earlier, the supernatant was discarded and the remaining pellet was resuspended in 500 μl of water. Next, 500 μl of an amylase reaction solution (50 mM MOPS-KOH, pH 6.5, 20 units α-amylase) was added to the samples, which were then incubated at 37°C for 2 h. After centrifugation, the resulting supernatant including starch was removed. The precipitate was once again suspended in 500 μl of water, boiled for 10 min, and centrifuged at 21 500*g* for 5 min at 4°C. The supernatant was collected as the hot water fraction. This step was repeated twice. Next, the same procedures were carried out using 50 mM EDTA (pH 8.0)/50 mM sodium phosphate buffer (pH 6.8) and 4 M KOH supplemented with 10.6 mM $NaBH_4$. The supernatants obtained in each step were collected as the EDTA and KOH fractions. The KOH fraction was neutralized by adding glacial acetic acid. The precipitate was washed with water, ethanol, and diethyl ether and then air-dried overnight. The resulting powder was hydrolyzed in 100 μl of 72% sulfuric acid for 1 h and then in 800 μl of 8% sulfuric acid for 4 h. This final product was collected as the cellulose fraction. Sugar content was determined using the phenol–sulfuric acid method (DuBois et al. 1956).

Map-based cloning

In the F_2 population from two independent crosses of *sca* mutant (OUM206) with cv. Morex, 29.8% (78/262) of the plants displayed the short-awn phenotype associated with *sca*. This short-awn phenotype is linked to the semidwarf trait caused by the *uzu* gene on chromosome 3H. F_2 populations showed the segregation of *uzu* without *sca*, exhibiting semidwarfism as in cv. Akashinriki. The proportions of each phenotype are as follows: in the 159-plant F_2 population, Morex (long awn):*uzu* (semidwarf with moderately long awn):*sca* (short awn): OUM206 (*uzu sca*; semidwarf with extremely short awn) = 111:6:3:39; in the 103-plant F_2 population, the population was 66:1:5:31. In the F_2 population from a cross with cv. Harrington, 23.1% (80/342) of plants displayed the short-awn phenotype of *sca*. For mapping, publicly available markers and originally developed markers were used. Public SSR markers Bmac0067 and Bmag0603 (Varshney et al. 2007) and GBM1413 (Ramsay et al. 2000); CAPS markers k00879, k02775, k03628, k08560, and k09032 (Sato and Takeda 2009); and the dCAPS marker uzu_dCAPS (Saisho et al. 2004) were detected as described by Taketa et al. (2021). We originally developed markers using sequence information on syntenic rice chromosome 1 genes. Primers were designed based on homologous barley gene sequences (Morex V1 IBSCv2) obtained by Ensembl-Barley BLAST searches, using rice genes (RGAP database) as queries.

For deletion mapping, PCR using these primers was conducted to search for deletions harboring the *sca* locus from the panel of 27 *ari-a* mutants along with KM8. Genes within the candidate regions were amplified by PCR. The presence or absence of the expected bands was checked for each line to identify deletions. For some genes suspected to be near or within the deletion regions, we confirmed the sequences for select lines, such as Morex, Akashinriki, and *sca* mutant (OUM206), or for each line.

To test if the *sca* locus corresponds to the QTL AL4 in OUH602, phenotypic segregation of awn lengths was analyzed in the Harrington × OUH602 BC_1F_2 generation using *sca*-flanking markers k09032 and GBM1413. The BC_1F_2 population was derived from a heterozygous *sca* locus plant in the (Harrington × OUH602) × Harrington backcross. Homozygous Harrington and OUH602 alleles were selected using these markers, and awn lengths were measured at the fourth spikelet from the top.

Markers/primers for mapping are listed in Supplementary Table S4.

Subcellular localization analysis

To construct 35S::SCA–GFP, total RNA was extracted from inflorescences at W7.5 of BW using the RNeasy Plant Mini Kit (QIAGEN, Hilden, Germany). cDNA synthesis was performed using the PrimeScript II 1st Strand cDNA Synthesis Kit (Takara, Kusatsu, Japan). The 3741-bp full-length CDS of the *SCA* gene (excluding stop codons) was cloned into the pK7FWG2 binary vector via Gateway cloning (Invitrogen, Carlsbad, USA). To construct 35S::GFP, the sequence containing the stop codon was inserted into the pENTR/SD/D-TOPO vector (Invitrogen, Carlsbad, USA) and subsequently cloned into the pK7FWG2 binary vector via Gateway cloning. To construct 35S::mScarlet-I-H2B, the synthesized *mScarlet-I* sequence (699 bp; Eurofins Genomics Tokyo, Tokyo, Japan) was amplified by PCR and fused via recombinant PCR with the full-length CDS of *NbH2B* gene (444 bp), isolated from *N. benthamiana* as previously described (Hyodo et al. 2019). The resulting PCR product was then cloned into the pCAMBIA1300 binary vector containing the 35S promoter using In-Fusion HD cloning technology (Clontech, Mowntain View, USA). Transient expression in *N. benthamiana* leaves by infiltrating *Agrobacterium tumefaciens* (GV 3301) harboring these binary constructs was conducted as described previously (Hyodo et al. 2019). Fluorescence signals were captured after 36 h in the dark following infiltration, using a Fluoview FV1000-D microscope (Olympus, Tokyo, Japan). Primers are listed in Supplementary Table S5.

qRT-PCR

Spikes were harvested at W7.5 from BW, *sca*-BW, and *ari-a.6*-BW; at W8.5 from BW; and at W9.5 from BW. At W9.5, spikelets (excluding awns) from BW; awns from BW, *sca*-BW, and *ari-a.6*-BW; and flag leaves from BW were collected, all in three biological replicates. cDNA synthesis was performed using the PrimeScript RT Reagent Kit (Perfect Real Time; Takara, Kusatsu, Japan). The real-time PCR was performed with TB Green Premix Ex Taq II (Takara, Kusatsu, Japan) on a LightCycler 96 (Roche, Basel, Switzerland). Relative expression levels were calculated using the ΔΔCT method with *ACTIN* (*HORVU.MOREX.r3.1HG0003140*) as the internal control as in Trevaskis et al. (2006). Primers are listed in Supplementary Table S5.

Analysis of RNA sequencing

Inflorescences at W7.5 and elongated awns at the heading stage were collected in three batches for each genotype: BW, *ari-a.6*-BW, and *sca*-BW, except for *sca*-BW awn samples, which had two replicates. Total RNA was extracted using the RNeasy Plant Mini Kit (QIAGEN, Hilden, Germany), and quality was assessed

using the 2100 Bioanalyzer (Agilent Technologies, Santa Clara, USA). RNA-seq libraries were prepared using the KAPA mRNA Capture kit and sequenced on the DNBSEQ-G400RS platform (MGI, Shenzhen, China) with an average of 26 million paired-end 150-bp reads per library by Genome-Lead Co. (Kagawa, Japan). Reads were quality-checked and trimmed using Trimmomatic v0.39 (Bolger et al. 2014), aligned to the *H. vulgare* cv. MorexV3 reference genome using hisat2 v2.1.0 (Kim et al. 2019), and processed using SAMtools v1.9 (Li et al. 2009). Transcript assembly was conducted using StringTie v2.2.0 (Pertea et al. 2015), and gene read counts were generated using prepDE.py. Count per million (CPM) values were calculated using iDEP.96 (Ge et al. 2018), identifying 21 432 genes with more than 0.5 CPM in at least one sample. DEGs were identified with DESeq2 v1.36.0 (Love et al. 2014) using |Log2 fold change| > 1 and false discovery rate (FDR) < 0.05. GO enrichment analysis was performed using clusterProfiler v4.10.1 (Wu et al. 2021). The raw sequencing data for RNA-seq have been deposited in the DNA Data Bank of Japan/BioProject under accession number PRJDB18689. Data on *SCA* expression in barley organs were obtained from BarleyExpDB (http://barleyexp.com/) based on the SRA BioProject PRJEB14349 Study.

ChIP-qPCR

Two grams of elongated awns at the heading stage were collected in three biological replicates for each genotype: BW and *ari-a.6*-BW. The samples were cross-linked with 1% formaldehyde under vacuum for 10 min, quenched with 0.125 M glycine, and frozen in liquid nitrogen. Nuclear extraction and immunoprecipitation were performed using a modified protocol (Nozawa et al. 2022). Chromatin was resuspended in SDS lysis buffer and sonicated to 300- to 500-bp fragments using a Bioruptor sonicator (Diagenode, Liege, Belgium). Immunoprecipitation was done with a 100-fold dilution of mouse anti-H3K27me3 antibody (MABI0323, lot #18008; MAB Institute, Iida, Japan), followed by DNA elution. The samples were reverse cross-linked overnight at 65°C, then treated with proteinase K and RNase, and subsequently purified using the phenol–chloroform method. The pellets were resuspended in 15 μl of 1× TE and diluted 40-fold for real-time PCR. Real-time PCR was conducted using TB Green Premix Ex Taq II (Takara, Kusatsu, Japan) on LightCycler 96 (Roche, Basel, Switzerland). The "% of input" values were calculated using the ΔΔCT method, normalized to the input. The primers for ChIP-qPCR are listed in Supplementary Table S5.

Observation of spikelet and awn

Floral organs of spikelets at the green anther stage were observed using an MVX10 microscope (Olympus, Tokyo, Japan). Awns at 2 weeks after heading were sliced vertically and horizontally to approximately 1 mm thickness and observed under bright and UV light for autofluorescence. The dimensions of parenchymal cells were measured from longitudinal and cross-sectional images. The length of parenchyma cells within a ±5 mm range from the midpoint between the base and tip of the awns on middle spikelets was measured in the cell file adjacent to the chlorenchyma tissues. Awn observations were made using a BX-50 optical microscope (Olympus, Tokyo, Japan) equipped with an epifluorescence attachment. Spikelets at the W4.5 stage were observed using a Quanta 250 SEM (FEI, Hillsboro, USA).

Acknowledgments

The authors are grateful to H. Bockelman, U. Lundqvist, J. Franckowiack, and N. Kawada for supplying barley seeds. The barley resources were also provided by the National BioResource Project—Barley, Japan. We thank H. Hisano, D. Saisho, R. Matsushima, and Hirayama laboratory members for experimental support and helpful discussions.

Supplementary data

Supplementary data is available at *PCP* online.

Conflict of interest

None declared.

Funding

This work was supported by Grants-in-Aid for Scientific Research from the Japan Society for the Promotion of Science (22K06266 to Y.I., 23H04747 to Y.I., 25450008 to S.T., and 23K26877 to S.T.), the Ohara Foundation (to Y.I.), and Japan Science and Technology Agency SPRING (JPMJSP2126 to K.N.).

References

Anwar, N., Ohta, M., Yazawa, T., Sato, Y., Li, C., Tagiri, A., et al. (2018) miR172 downregulates the translation of cleistogamy 1 in barley. *Ann. Bot.* 122: 251–265.

Aubert, D., Chen, L., Moon, Y.-H., Martin, D., Castle, L.A., Yang, C.-H., et al. (2001) EMF1, a novel protein involved in the control of shoot architecture and flowering in Arabidopsis. *Plant Cell* 13: 1865–1875.

Becker, A. and Theißen, G. (2003) The major clades of MADS-box genes and their role in the development and evolution of flowering plants. *Mol. Phylogenet. Evolut., Plant Mol. Evolut.* 29: 464–489.

Bessho-Uehara, K., Masuda, K., Wang, D.R., Angeles-Shim, R.B., Obara, K., Nagai, K., et al. (2023) *Regulator of Awn Elongation* 3, an E3 ubiquitin ligase, is responsible for loss of awns during African rice domestication. *Proc. Natl. Acad. Sci. U.S.A.* 120: e2207105120.

Bessho-Uehara, K., Wang, D.R., Furuta, T., Minami, A., Nagai, K., Gamuyao, R., et al. (2016) Loss of function at *RAE2*, a previously unidentified EPFL, is required for awnlessness in cultivated Asian rice. *Proc. Natl. Acad. Sci. U.S.A.* 113: 8969–8974.

Bolger, A.M., Lohse, M. and Usadel, B. (2014) Trimmomatic: a flexible trimmer for Illumina sequence data. *Bioinformatics* 30: 2114–2120.

Calonje, M., Sanchez, R., Chen, L. and Sung, Z.R. (2008) EMBRYONIC FLOWER1 participates in polycomb group–mediated AG gene silencing in Arabidopsis. *Plant Cell* 20: 277–291.

Causier, B., Schwarz-Sommer, Z. and Davies, B. (2010) Floral organ identity: 20 years of ABCs. *Semin. Cell Dev. Biol. Tumor-Stroma Interact.* 21: 73–79.

Chen, G., Mishina, K., Wang, Q., Zhu, H., Tagiri, A., Kikuchi, S., et al. (2023) Organ-enriched gene expression during floral morphogenesis in wild barley. *Plant J.* 116: 887–902.

Chono, M., Honda, I., Zeniya, H., Yoneyama, K., Saisho, D., Takeda, K., et al. (2003) A semidwarf phenotype of barley uzu results from a nucleotide substitution in the gene encoding a putative brassinosteroid receptor. *Plant Physiol.* 133: 1209–1219.

Ciaffi, M., Paolacci, A.R., Tanzarella, O.A. and Porceddu, E. (2011) Molecular aspects of flower development in grasses. *Sex Plant Reprod.* 24: 247–282.

Coen, E.S. and Meyerowitz, E.M. (1991) The war of the whorls: genetic interactions controlling flower development. *Nature* 353: 31–37.

DeWitt, N., Guedira, M., Lauer, E., Sarinelli, M., Tyagi, P., Fu, D., et al. (2020) Sequence-based mapping identifies a candidate transcription repressor underlying awn suppression at the B1 locus in wheat. *New Phytologist* 225: 326–339.

Druka, A., Franckowiak, J., Lundqvist, U., Bonar, N., Alexander, J., Houston, K., et al. (2011) Genetic dissection of barley morphology and development. *Plant Physiol.* 155: 617–627.

Du, D., Zhang, D., Yuan, J., Feng, M., Li, Z., Wang, Z., et al. (2021) FRIZZY PANICLE defines a regulatory hub for simultaneously controlling spikelet formation and awn elongation in bread wheat. *New Phytologist* 231: 814–833.

DuBois, M., Gilles, K.A., Hamilton, J.K., Rebers, P.A. and Smith, F. (1956) Colorimetric method for determination of sugars and related substances. *Anal. Chem*. 28: 350–356.

Ge, S.X., Son, E.W. and Yao, R. (2018) iDEP: an integrated web application for differential expression and pathway analysis of RNA-Seq data. *BMC Bioinf*. 19: 534.

Grundbacher, F.J. (1963) The physiological function of the cereal awn. *Bot. Rev*. 29: 366–381.

Gu, B., Zhou, T., Luo, J., Liu, H., Wang, Y., Shangguan, Y., et al. (2015) An-2 encodes a cytokinin synthesis enzyme that regulates awn length and grain production in rice. *Mol. Plant* 8: 1635–1650.

Gyenis, L., Yun, S.J., Smith, K.P., Steffenson, B.J., Bossolini, E., Sanguineti, M.C., et al. (2007) Genetic architecture of quantitative trait loci associated with morphological and agronomic trait differences in a wild by cultivated barley cross. *Genome* 50: 714–723.

Hagen, G. and Guilfoyle, T. (2002) Auxin-responsive gene expression: genes, promoters and regulatory factors. *Plant Mol. Biol*. 49: 373–385.

Heery, D.M., Kalkhoven, E., Hoare, S. and Parker, M.G. (1997) A signature motif in transcriptional co-activators mediates binding to nuclear receptors. *Nature* 387: 733–736.

Hua, L., Wang, D.R., Tan, L., Fu, Y., Liu, F., Xiao, L., et al. (2015) *LABA1*, a domestication gene associated with long, barbed awns in wild rice. *Plant Cell* 27: 1875–1888.

Huang, B., Wu, W. and Hong, Z. (2021) Genetic loci underlying awn morphology in barley. *Genes* 12: 1613.

Huang, D., Zheng, Q., Melchkart, T., Bekkaoui, Y., Konkin, D.J.F., Kagale, S., et al. (2020) Dominant inhibition of awn development by a putative zinc-finger transcriptional repressor expressed at the B1 locus in wheat. *New Phytologist* 225: 340–355.

Hyodo, K., Suzuki, N. and Okuno, T. (2019) Hijacking a host scaffold protein, RACK1, for replication of a plant RNA virus. *New Phytologist* 221: 935–945.

Kim, D., Paggi, J.M., Park, C., Bennett, C. and Salzberg, S.L. (2019) Graph-based genome alignment and genotyping with HISAT2 and HISAT-genotype. *Nat. Biotechnol*. 37: 907–915.

Kim, S.Y., Lee, J., Eshed-Williams, L., Zilberman, D., Sung, Z.R. and Reed, J.W. (2012) EMF1 and PRC2 cooperate to repress key regulators of Arabidopsis development. *PLoS Genet*. 8: e1002512.

Kim, S.Y., Zhu, T. and Sung, Z.R. (2010) Epigenetic regulation of gene programs by EMF1 and EMF2 in Arabidopsis. *Plant Physiol*. 152: 516–528.

Kjack, J.L. and Witters, R.E. (1974) Physiological activity of awns in isolines of atlas barley. *Crop Sci*. 14: 243–248.

Konishi, T., Hayashi, J., Moriya, I. and Takahashi, R. (1984) Inheritance and linkage studies in barley VII. Location of six new mutant genes on chromosome 3. *Ber. Ohara Inst. Landw. Biol*. 18: 251–264.

Kucera, J., Lundqvist, U. and Gustafsson, A. (1975) Induction of breviaristatum mutants in barley. *Hereditas* 80: 263–277.

Kuijer, H.N.J., Shirley, N.J., Khor, S.F., Shi, J., Schwerdt, J., Zhang, D., et al. (2021) Transcript profiling of MIKCc MADS-box genes reveals conserved and novel roles in barley inflorescence development. *Front. Plant Sci*. 12: 705286.

Kutsuno, T., Chowhan, S., Kotake, T. and Takahashi, D. (2023) Temporal cell wall changes during cold acclimation and deacclimation and their potential involvement in freezing tolerance and growth. *Physiol. Plant*. 175: e13837.

Li, G., Kuijer, H.N.J., Yang, X., Liu, H., Shen, C., Shi, J., et al. (2021) MADS1 maintains barley spike morphology at high ambient temperatures. *Nat. Plants* 7: 1093–1107.

Li, H., Handsaker, B., Wysoker, A., Fennell, T., Ruan, J., Homer, N., et al. (2009) The sequence alignment/map format and SAMtools. *Bioinformatics* 25: 2078–2079.

Li, H., Liang, W., Jia, R., Yin, C., Zong, J., Kong, H., et al. (2010) The AGL6-like gene OsMADS6 regulates floral organ and meristem identities in rice. *Cell Res*. 20: 299–313.

Liller, C.B., Walla, A., Boer, M.P., Hedley, P., Macaulay, M., Effgen, S., et al. (2017) Fine mapping of a major QTL for awn length in barley using a multiparent mapping population. *Theor. Appl. Genet*. 130: 269–281.

Liu, X., Yang, C.Y., Miao, R., Zhou, C.L., Cao, P.H., Lan, J., et al. (2018) DS1/OsEMF1 interacts with OsARF11 to control rice architecture by regulation of brassinosteroid signaling. *Rice* 11: 46.

Love, M.I., Huber, W. and Anders, S. (2014) Moderated estimation of fold change and dispersion for RNA-seq data with DESeq2. *Genome Biol*. 15: 550.

Luo, J., Liu, H., Zhou, T., Gu, B., Huang, X., Shangguan, Y., et al. (2013) An-1 encodes a basic helix-loop-helix protein that regulates awn development, grain size, and grain number in rice. *Plant Cell* 25: 3360–3376.

Moriya, I. and Takahashi, R. (1980) Linkage studies of three barley mutants. *Barley Gen. Newsl*. 10: 47–51.

Müller, K.J., Romano, N., Gerstner, O., Garcia-Marotot, F., Pozzi, C., Salamini, F., et al. (1995) The barley Hooded mutation caused by a duplication in a homeobox gene intron. *Nature* 374: 727–730.

Murai, K. (2013) Homeotic genes and the ABCDE model for floral organ formation in wheat. *Plants* 2: 379–395.

Nagasawa, N., Miyoshi, M., Sano, Y., Satoh, H., Hirano, H., Sakai, H., et al. (2003) SUPERWOMAN1 and DROOPING LEAF genes control floral organ identity in rice. *Development* 130: 705–718.

Nozawa, K., Masuda, S., Saze, H., Ikeda, Y., Suzuki, T., Takagi, H., et al. (2022) Epigenetic regulation of ecotype-specific expression of the heat-activated transposon ONSEN. *Front. Plant Sci*. 13: 899105.

Patil, V., McDermott, H.I., McAllister, T., Cummins, M., Silva, J.C., Mollison, E., et al. (2019) APETALA2 control of barley internode elongation. *Development* 146: dev170373.

Pertea, M., Pertea, G.M., Antonescu, C.M., Chang, T.-C., Mendell, J.T. and Salzberg, S.L. (2015) StringTie enables improved reconstruction of a transcriptome from RNA-seq reads. *Nat. Biotechnol*. 33: 290–295.

Ramsay, L., Macaulay, M., Ivanissevich, S.D., MacLean, K., Cardle, L., Fuller, J., et al. (2000) A simple sequence repeat-based linkage map of barley. *Genetics* 156: 1997–2005.

Ranocha, P., Dima, O., Nagy, R., Felten, J., Corratgé-Faillie, C., Novák, O., et al. (2013) Arabidopsis WAT1 is a vacuolar auxin transport facilitator required for auxin homoeostasis. *Nat. Commun*. 4: 2625.

Richardson, A., Rebocho, A.B. and Coen, E. (2016) Ectopic KNOX expression affects plant development by altering tissue cell polarity and identity. *Plant Cell* 28: 2079–2096.

Saisho, D., Tanno, K., Chono, M., Honda, I., Kitano, H. and Takeda, K. (2004) Spontaneous brassinolide-insensitive barley mutants *uzu* adapted to East Asia. *Breed. Sci*. 54: 409–416.

Sato, K. and Takeda, K. (2009) An application of high-throughput SNP genotyping for barley genome mapping and characterization of recombinant chromosome substitution lines. *Theor. Appl. Genet*. 119: 613–619.

Sun, M., Jiang, C., Gao, G., An, C., Wu, W., Kan, J., et al. (2024) A novel type of malformed floral organs mutant in barley was conferred by loss-of-function mutations of the MADS-box gene HvAGL6. *Plant J*. 119: 2609–2621.

Sung, Z.R., Belachew, A., Shunong, B. and Bertrand-Garcia, R. (1992) EMF, an Arabidopsis gene required for vegetative shoot development. *Science* 258: 1645–1647.

Takahashi, R. (1955) The origin and evolution of cultivated barley. *Adv. Genet*. 7: 227–266.

Takanashi, H., Kajiya-Kanegae, H., Nishimura, A., Yamada, J., Ishimori, M., Kobayashi, M., et al. (2022) *DOMINANT AWN INHIBITOR* encodes the ALOG protein originating from gene duplication and inhibits awn elongation by suppressing cell proliferation and elongation in sorghum. *Plant Cell Physiol*. 63: 901–918.

Taketa, S., Hattori, M., Takami, T., Himi, E. and Sakamoto, W. (2021) Mutations in a *Golden2-Like* gene cause reduced seed weight in barley *albino lemma 1* mutants. *Plant Cell Physiol*. 62: 447–457.

Tanaka, W., Toriba, T., Ohmori, Y., Yoshida, A., Kawai, A., Mayama-Tsuchida, T., et al. (2012) The *YABBY* Gene *TONGARI-BOUSHI1* is involved in lateral organ development and maintenance of meristem organization in the rice spikelet. *Plant Cell* 24: 80–95.

Toriba, T. and Hirano, H.-Y. (2014) The DROOPING LEAF and OsETTIN2 genes promote awn development in rice. *Plant J*. 77: 616–626.

Trevaskis, B., Hemming, M.N., Peacock, W.J. and Dennis, E.S. (2006) HvVRN2 responds to daylength, whereas HvVRN1 is regulated by vernalization and developmental status. *Plant Physiol*. 140: 1397–1405.

Tsuda, K., Maeno, A., Otake, A., Kato, K., Tanaka, W., Hibara, K.-I., et al. (2024) YABBY and diverged KNOX1 genes shape nodes and internodes in the stem. *Science* 384: 1241–1247.

Varshney, R.K., Marcel, T.C., Ramsay, L., Russell, J., Röder, M.S., Stein, N., et al. (2007) A high density barley microsatellite consensus map with 775 SSR loci. *Theor. Appl. Genet*. 114: 1091–1103.

von Bothmer, R., Jacobsen, N., Baden, C., Jørgensen, R.B. and Linde-Laursen, I. (1995) An ecogeographical study of the genus Hordeum, systematic and ecogeographic studies on crop genepools. *Rome: Int. Plant Genet. Resour. Inst*. 7: 129.

Waddington, S.R., Cartwright, P.M. and Wall, P.C. (1983) A quantitative scale of spike initial and pistil development in barley and wheat. *Ann. Bot*. 51: 119–130.

Wang, Y., Gu, X., Yuan, W., Schmitz, R.J. and He, Y. (2014) Photoperiodic control of the floral transition through a distinct polycomb repressive complex. *Dev. Cell* 28: 727–736.

Weigel, D. and Meyerowitz, E.M. 1994 The ABCs of floral homeotic genes. *Cell* 78: 203–209.

Wu, T., Hu, E., Xu, S., Chen, M., Guo, P., Dai, Z., et al. (2021) clusterProfiler 4.0: A universal enrichment tool for interpreting omics data. *The Innovation*. 2: 100141.

Yamaguchi, T., Nagasawa, N., Kawasaki, S., Matsuoka, M., Nagato, Y. and Hirano, H.-Y. (2004) The *YABBY* gene *DROOPING LEAF* regulates carpel specification and midrib development in *Oryza sativa*. *Plant Cell* 16: 500–509.

Yan, D., Zhang, X., Zhang, L., Ye, S., Zeng, L., Liu, J., et al. (2015) CURVED CHIMERIC PALEA 1 encoding an EMF1-like protein maintains epigenetic repression of OsMADS58 in rice palea development. *Plant J*. 82: 12–24.

Yasui, Y., Ohmori, Y., Takebayashi, Y., Sakakibara, H., Hirano, H.-Y. and Hake, S. (2018) WUSCHEL-RELATED HOMEOBOX4 acts as a key regulator in early leaf development in rice. *PLoS Genet*. 14: e1007365.

Yin, X., Romero-Campero, F.J., de Los Reyes, P., Yan, P., Yang, J., Tian, G., et al. (2021) H2AK121ub in Arabidopsis associates with a less accessible chromatin state at transcriptional regulation hotspots. *Nat. Commun*. 12: 315.

Yoshida, H. and Nagato, Y. (2011) Flower development in rice. *J. Exp. Bot*. 62: 4719–4730.

Yuo, T., Yamashita, Y., Kanamori, H., Matsumoto, T., Lundqvist, U., Sato, K., et al. (2012) A SHORT INTERNODES (SHI) family transcription factor gene regulates awn elongation and pistil morphology in barley. *J. Exp. Bot*. 63: 5223–5232.

Zhang, D., Guo, W., Wang, T., Wang, Y., Le, L., Xu, F., et al. (2023) RNA 5-methylcytosine modification regulates vegetative development associated with H3K27 trimethylation in Arabidopsis. *Adv. Sci*. 10: 2204885.

Zhang, Y., Shen, C., Li, G., Shi, J., Yuan, Y., Ye, L., et al. (2024) MADS1-regulated lemma and awn development benefits barley yield. *Nat. Commun*. 15: 301.

Zheng, M., Wang, Y., Wang, Y., Wang, C., Ren, Y., Lv, J., et al. (2015) DEFORMED FLORAL ORGAN1 (DFO1) regulates floral organ identity by epigenetically repressing the expression of OsMADS58 in rice (Oryza sativa). *New Phytologist* 206: 1476–1490.

Zhou, L., Zhu, C., Fang, X., Liu, H., Zhong, S., Li, Y., et al. (2021) Gene duplication drove the loss of awn in sorghum. *Mol. Plant* 14: 1831–1845.